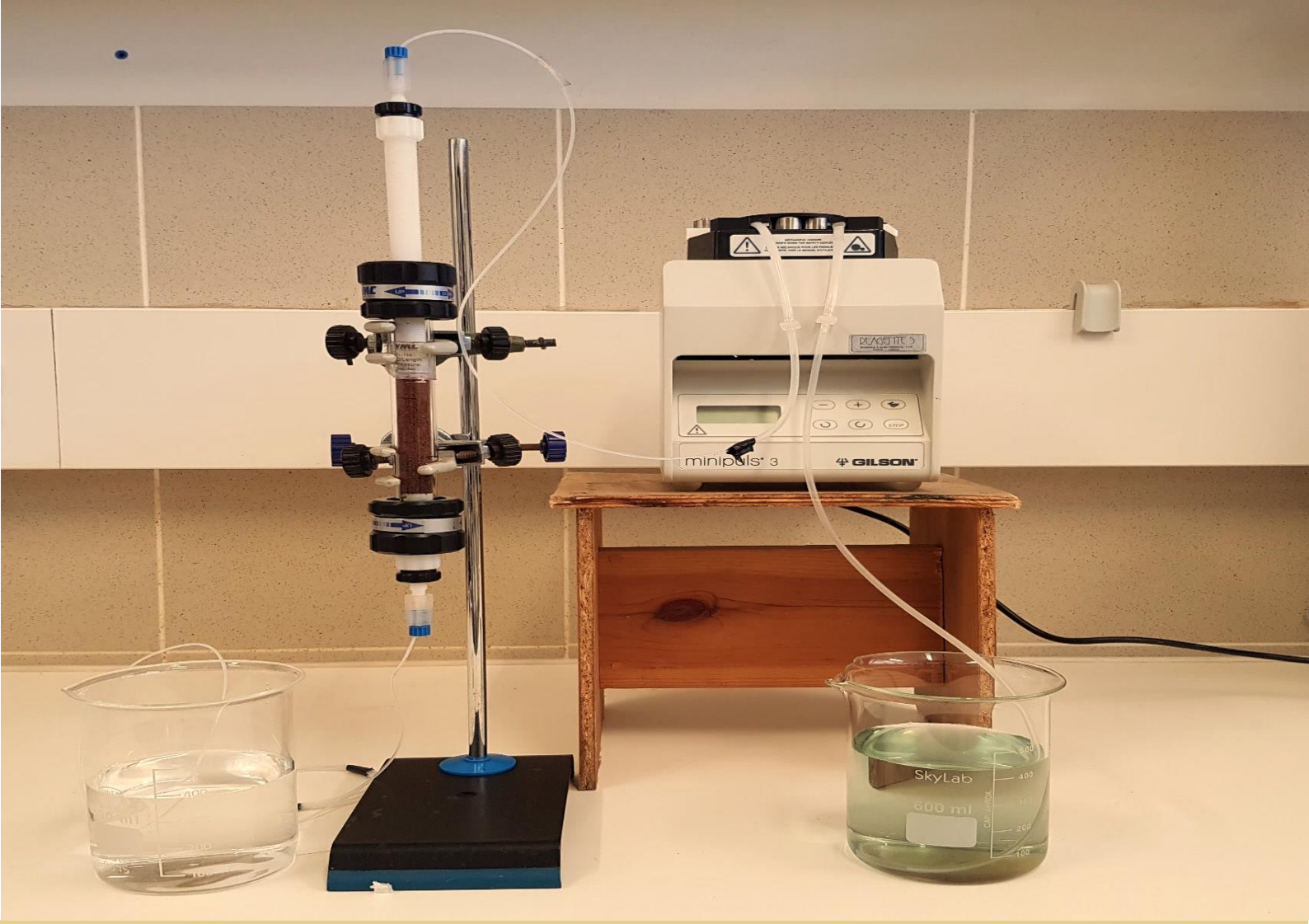

Kevin Neves

Sorption of Cr(III) in fixed-bed column by modified pine bark: optimization and modelling studies

Master's thesis in the scientific area of Chemical Engineering, supervised by *Professor Doctor Licínio Ferreira* and *Professor Doctor Margarida Quina* and submitted to the Department of Chemical Engineering, Faculty of Science and Technology, University of Coimbra

September 2017

UNIVERSIDADE DE COIMBRA

Kevin Neves

Sorption of Cr(III) in fixed-bed column by modified pine bark: optimization and modelling studies

Master Thesis in the scientific area of Chemical Engineering and submitted to the Department of Chemical Engineering, Faculty of Science and Technology, University of Coimbra

Supervisor(es)/Supervisor(s):

Prof. Dr. Licínio Manuel Gando de Azevedo Ferreira

Prof. Dr. Margarida Maria João de Quina

Host institutions:

CIEPQPF - Research Centre for Chemical Processes Engineering and Forest Products, Department of Chemical Engineering, Faculty of Sciences and Technology of the University of Coimbra

Coimbra, September 2017

UNIVERSIDADE DE COIMBRA

ACKNOWLEDGEMENTS

The time has come, one more step completed. It is time to embrace the future, enter in a new world of discoveries and challenges. It's time to look into the past with a smile on my face remembering all the moments I've pass through.

First of all, I want to thank my parents and my grandmother for all the support, help and encouragement along this path, without them it would not be possible. To my uncles, to my godmother Joana and to my grandparents also a sincere gratitude.

To my supervisors, Professor Doctor Licínio Ferreira and Professor Doctor Margarida Quina my deepest acknowledgment for all the support, availability and guidance in all the moments during this project.

To Aline for her kindness, availability, cooperation, guidance and advice during this semester at the laboratory and also outside of it.

To my university family: Rita, Xana, Joana, Priscila, Vera, Miguel, Rodrigo, Dani and Joli who have been always there for all the moments and for their friendship. Without them, it would be much harder.

To all my friends of Mala who always believed in me, for their friendship and all the moments that we've passed.

To all the Professors of the Chemical Engineering Department of the University of Coimbra who provided me all the knowledge necessary to complete this course.

To all of you, my deepest and sincere acknowledgment!

ABSTRACT

The adsorption process in fixed bed columns, is one of the most advantageous processes for the removal of heavy metals, allowing the treatment of large volumes of effluent. The fact that the bed can be regenerated and the possibility of being reused allowing the recover the adsorbed metal are other factors in favor of its use in large-scale industrial processes. Chromium is the heavy metal selected in this study, because of its relevance in the electroplating, coating and tanning industries. The effluents from these industries may contain detrimental concentrations of Cr.

This work, aims to analyse the dynamic behavior of a fixed bed column, in which the adsorbent was prepared in the lab. Following the previous work, mercerized pine bark (MPB) will be used as adsorbent to remove Cr (III) and to purify a synthetic effluent. Thus, operational parameters such as bed height, fluid velocity and effluent inlet concentration were tested to obtain the maximum saturated bed fraction and to predict the behavior of the adsorption process for each case. A mechanistic model was developed for predicting the behaviour of the fixed bed, that includes equilibrium parameters and the Linear Driving Force (LDF) approach to express the intraparticular mass transport. For an inlet concentration of 100 mg/L, the maximum saturated bed fraction was 0.65, obtained for the case where a height of 6.5 cm and a superficial velocity of 14.43×10^{-2} cm/s is used. Moreover, the influence of the same parameters was also studied to minimize the difference between the exhaust time and the break time of the column. In this case, using an inlet concentration of 100 mg/L, a bed height of 2.5 cm and a surface speed of 14.43×10^{-2} cm/s, were the best conditions.

Moreover, a Box-Benken-Design was used to determine the most influent inlet variables (factors) on adsorption efficiency. By using multiple linear regression, empirical models were developed and the optimal operating conditions to maximize the saturated bed fraction were identified. Finally, a regeneration of the adsorbent material was assessed through two chemical agents (nitric acid and N,N-Bis(carboxymethyl)-DL-alanine trisodium salt).

From this study, it was possible to conclude that the biosorbent tested can be used in fixed-bed column process for remove chromium from liquid effluents.

Keywords: Adsorption, chromium, fixed-bed column, modified pine bark, mechanistic model, Box-Benken-Design, regeneration.

RESUMO

O processo de adsorção, utilizando colunas de leito fixo, mostra-se como um dos processos mais vantajosos para a remoção de metais pesados de efluentes industriais. O facto de o leito poder ser regenerado, haver a possibilidade de ser reutilizado e recuperar o metal adsorvido são outros fatores a favor para o seu uso. O crómio, por ser utilizado em processos de galvanoplastia, revestimentos e curtumes, ocorre frequentemente no meio ambiente devido aos efluentes provenientes deste tipo de indústrias.

Neste trabalho será estudado o comportamento dinâmico de uma coluna de leito fixo em que o adsorvente utilizado foi obtido no laboratório a partir de casca de pinheiro. No seguimento de trabalhos anteriores, este material, será utilizado como adsorvente para remover o Cr(III). Foram realizadas várias experiências para testar diversos parâmetros operacionais, como a altura do leito, a velocidade superficial do fluido e a concentração de entrada do efluente. Na prática pretende-se obter a máxima fração de leito saturado e prever o comportamento dinâmico do processo de adsorção. Um modelo de natureza mecanística foi desenvolvido de modo a prever a resposta do sistema face a variações dos parâmetros operacionais. Foram incluídas as relações de equilíbrio bem como o modelo Linear Driving Force (LDF) para expressar o transporte de massa intraparticular. Deste modo verificou-se que, para uma concentração de entrada fixa em 100 mg/L, a máxima fração de leito saturado obtida é de 0.65, para o caso onde se utilizada uma altura de leiro de 6,5 cm e uma velocidade superficial de 14.43×10^{-2} cm/s. Foi também estudado a influência dos mesmos parâmetros de modo a minimizar a diferença entre o tempo de exaustão onde as condições ótimas são uma altura de leito de 2,5 cm e uma velocidade superficial de 14.43×10^{-2} cm/s

Para além disto, desenho fatorial do tipo Box-Benken-Design foi utilizado de modo a determinar quais as variáveis que mais influenciam a eficiência do processo de adsorção em leito fixo. Utilizando uma regressão linear múltipla, dois modelos empíricos foram construídos onde foram identificas as condições ótimas de operação de modo a maximizar a fração de leito saturado. Por fim, a regeneração do adsorvente foi feita utilizando dois agentes químicos (ácido nítrico e *N,N-Bis(carboxymethyl)-DL-alanine trisodium salt*).

Assim, deste estudo foi possível concluir que o adsorvente testado pode ser utilizado em processos com colunas de leito fixo para a remoção de crómio de efluentes líquidos.

Palavras chave: Adsorção, crómio, coluna de leito fixo, casca de pinheiro modificada, modelo mecanístico, Box-Benken Design, regeneração.

INDEX

LIST OF FIGURES

LIST OF TABLES

NOMENCLATURE

A_s	Surface area (m^2)
C	Concentration (mg/L)
C_b	Bulk concentration (mg/L)
C_E	Feed concentration of the adsorbate (mg/L)
C_s	Surface concentration (mg/L)
D_{ax}	Axial dispersion coefficient (m^2/s)
D_m	Molecular diffusivity (m^2/s)
D_{pe}	Effective pore diffusivity (m^2/min)
d_p	Particle diameter (m)
f_h	Humidity factor
H	Height of the bed (cm)
J	Mass transfer flux (kg/m^2s)
K_f	Freundlich isotherm constant ($mg^{(1/n)}\ L^{1/n}/g$)
K_L	Langmuir isotherm constant (L/mg)
k_{LDF}	LDF kinetic constant
m_{ads}	Mass of adsorbent (g)
m_d	Mass of the dried material (g)
m_i	Mass of initial material (g)
m_{na}	Not adsorbed mass (mg)
m_{total}	Total mass introduced (mg)
N	Flux of mass ($g/m^2.s$)
n	Freundlich isotherm constant
Q	Flow rate (mL/min)
q	Adsorption capacity (mg/g)
q^*	Adsorption capacity at the equilibrium (mg/g)
q_m	Maximum adsorptive capacity (mg/g)
$\langle q \rangle$	Average adsorbed phase concentration (mol/kg)
Re	Number of Reynolds
R^2	Determination coefficient
T_b	Bulk temperature
T_S	Surface temperature

t	Time (min)
t_{bp}	Breakthrough time (min)
t_E	Exhaustion time (min)
t_{st}	Stoichiometric time (min)
t_f	Total operation time (min)
u_0	Superficial velocity (m/s)
u_i	Interstitial velocity (m/s)
V	Volume (mL)
Z	Ion valence
Z	Bed length (m)
ε	Bed porosity
ε_p	Particle porosity
τ	Residence time (min)
ξ	Capacity factor
ρ_p	Particle density (kg/m^3)
η	Viscosity (Pa. s)
ΔH	Enthalpy (J)
Ω	LDF factor
λ	Conductance
τ	Tortuosity

ACRONYMS

BBD	Box-Benken design
DLS	Dynamic Light Scattering
DOE	Design of experiments
EDXRF	Elemental Analysis by Energy-Dispersive X-Ray Fluorescence
FLS	Saturated bed fraction
LDF	Linear Driving Force
MCL	Maximum concentration limits (mg/L)
MPB	Mercerized pine bark
MTZ	Mass transference zone

1. INTRODUCTION

1.1 Work motivation and scope

Chromium is considered a heavy metal and exists in nature in various oxidation states (di-, tri-, penta- and -hexa), however, Cr(III) and Cr(VI) are the most stable forms in the aquatic environment. With the increase of the industrial activities, the environmental pollution has increased as well. Thus, industrial effluents from the metal extraction and fabrication, leather tanning facilities, coating factories, pigments, electroplating, may contain high concentrations of chromium. Due to its carcinogenic and mutagenic properties, Cr(VI) is considered a highly toxic metal.[1,2]

Therefore, it is necessary to remove chromium from the environment and to control and treat the industrial outputs before being discharged into the water bodies.

There are several methods and techniques including chemical precipitation, reverse osmose, ion exchange, evaporation, flotation and electrodeposition that can remove chromium from wastewaters. However, they have considerable disadvantages such the high reagent and energy consumption, incomplete metal removal, generation of sludge or waste that requires special disposals and the expensive equipment and monitoring system.[3] Besides this, these methods are ineffective at lower concentrations of metal ions.

Recently, agricultural by-products and waste materials have received growing attention as an innovative and economical technology in removing heavy metals instead of the conventional methods. Lignocellulosic materials, particularly wood residues, have a great sorption capacity for chromium, comparable to the other natural or waste sorbents and they have the advantage of easily recovering and its cost is very low.[4]

In previous research, modified pine bark (MPB) was used as an adsorbent for the removal of Cr(III) from aqueous solutions in batch experiments. The obtained results showed that modified pine bark has an interesting adsorption capacity for the removal of this heavy metal.

However, for industrial applications of chromium ion removal, a continuous system is needed. In this thesis, in a fixed-bed column was investigated for the removal of Cr(III) with modified pine bark as an adsorbent.

1.2 Thesis objective

This thesis will be focused on the optimization of sorption of Cr(III) from synthetic effluent, in a fixed-bed column using modified pine bark.

The adsorbent material used in this experiences were characterized in a previous work. So, the main goal will be the study of the operational parameters effect (such as the superficial velocity, the bed depth and the feed concentration) on the adsorption efficiency using a laboratory scale fixed-bed column. Therefore, a design of experiments (DOE) will be used to identify and understand the influence of the parameters in the global system. Moreover, a multiple linear regression model will be obtained.

For predicting the dynamic response of the fixed-bed column, a mechanistic model will be developed, including the Linear Driving Force (LDF) model to account the intraparticular mass transfer. This model will be solved on MATLAB and will allow the comparison of the experimental results with the simulation predictions.

Finally, a regeneration test will be carried out aiming at reuse in new cycles of saturation.

1.3 Thesis structure

The present work is organized in 6 chapters. The first chapter includes the introduction where it is explained the scope of the study, the objective and the structure of the dissertation.

The second chapter contains the theoretical background and the fundamentals of the adsorption/desorption processes, adsorbents, the concepts and the mathematical models of fixed bed adsorption. In the third chapter is present the state of the art where are referenced general rate adsorption models and empirical models for dynamic fixed bed columns and a literature review. The experimental procedure and the methodologies used during the experiments are described in the fourth chapter. The experimental results and the models for describing the fixed-bed adsorption process are present and discussed in the fifth chapter.

At the end, in the sixth chapter, the final conclusions of the present work and some suggestions for future work are indicated.

2. THEORETICAL BACKGROUND

2.1 Heavy metals as contaminants for the environment

Since the beginning of industrialization, pollutants have been introduced into natural environments due to technological difficulties or lack of knowledge about the harmful impact. In particular, heavy metals are examples of pollutants that, in this case, are released into the ecosystems.[5] Heavy metals exist in nature mainly in ore minerals. However, their hazardousness to the public health and environment are mainly due to anthropogenic sources and the entry in the food chain.

The threat posed by heavy metals to the health of living organisms and plants is worsened because they are persistent and bioaccumulate contaminants, especially on aquatic environments.[1]

The most common heavy metals are iron (Fe), lead (Pb), copper (Cu), mercury (Hg), zinc (Zn), nickel (Ni) and chromium (Cr)[6]. Although some of these heavy metals are indispensable to life of all living beings, even at lower concentrations, they may have extremely bad effects due to their toxicity, cancerogenic properties and the ability to cause irritation and inflammation.[7]

Nowadays discharge limits for hazardous chemicals have been established for effluents, which have to be respected by the industries in order to minimize human and environmental exposure. Table 2.1 shows the maximum concentration limits (MCL) of heavy metals allowed to be discharged by the industries and the associated health hazards related to each one, reported by USEPA (United States Environmental Protection Agency).

Table 2.1: The maximum concentration limits for hazardous heavy metals in industrial effluents- (adapted from[8]).

Heavy metal	**Associated health hazards**	**MCL (mg/L)**
As	Skin manifestations, visceral cancers, vascular disease	0.050
Cd	Kidney damage, renal disorder, human carcinogen	0.01
Cr	Headache, diarrhea, nausea, vomiting, carcinogenic	0.05
Cu	Liver damage, Wilson disease, insomnia	0.25
Ni	Dermatitis, nausea, chronic asthma, coughing, human carcinogen	0.20
Zn	Depression, lethargy, neurological signs and increased thirst	0.80
Pb	Brain damage, diseases of the kidneys, circulatory and nervous system	0.006
Hg	Rheumatoid arthritis, diseases of the kidneys, circulatory and nervous system	0.00003

MCL- Maximum concentration limit.

Examples of natural processes that bring the heavy metals in the environment are erosion, volcanic eruptions, and the weathering of minerals.[9]

Heavy metals from anthropogenic sources, such as from chemical industry, typically have a high bioavailability due to their soluble and reactive forms. These anthropogenic sources include the production of alloys, batteries production, coating processes, explosive manufacturing, leather tanning, improper stacking of industrial solid waste, mining, phosphate fertilizer, pesticides, photographic materials, sewage irrigation, smelting, steel and electroplating industries, printing pigments, textiles, and wood preservation.[9,10]

Chromium, specifically, is very resistant to corrosion and it can be found in nature in form the of ferric chromite ore ($FeCr_2O_4$), crocoite, ($PbCrO_4$) and chrome ochre (Cr_2O_3).[9] Chromium has many oxidation states but the most common are chromium (III) and chromium (VI).

Due to their different oxidation states, this heavy metal possesses different toxicities being the Cr(VI) much more toxic compared to the other oxidation states.[1]

The form that this metal appears in nature is highly influenced by the pH and oxidation-reduction potential of the aquatic environment. Usually, the form Cr(III) appears as stable complexes or in its cationic form, while Cr(VI) appears in anionic form as a chromate (CrO_4^{2-}) or dichromate ($Cr_2O_7^{2-}$) or in acid form ($HCrO^{4-}$).[11]

The speciation of chromium as a function of the pH is represented in Figure 2.1. Is it possible to observe that until the pH of 3, the dominant speciation is Cr(III) and it appears as Cr^{3+}. As the pH increases, from 4 to 10 the most common species is ($Cr(OH)_2^+$). However, between the pH of 6 to 10, chromium may precipitate as $Cr(OH)_3$. Besides this, above pH of 10 chromium becomes soluble again in the form of ($Cr(OH)_4^-$).[12]

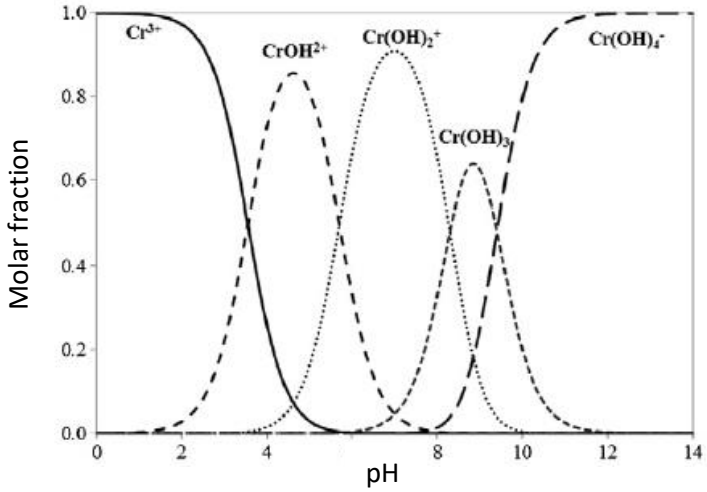

Figure 2.1: Speciation of chromium (III) at a given pH- (adapted from[12]) .

Analyzing the Pourbaix diagram, Figure 2.2, is another method to determine, at a given pH, which forms chromium takes place in an aqueous solution. This potential-pH diagram can be interpreted as a phase diagram, where the lines represent the frontiers between the stability areas of the different ionic species.

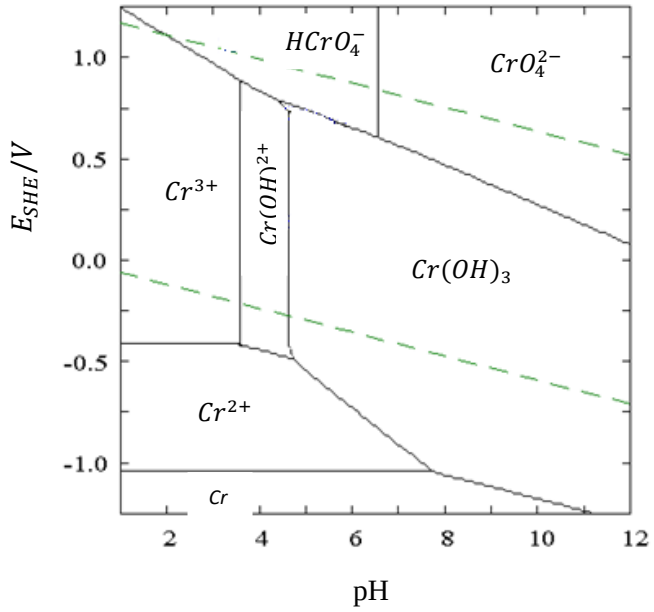

Figure 2.2: Pourbaix diagram for chromium at T=25 ºC in an aqueous solution [Cr(III)]=10^{-6} M- (adapted from[11]).

During the dissolution of Cr(III) salts, hydrolysis reactions can occur, and a reduction of pH values is normally observed by the following equations:

$$Cr^{3+} + H_2O \leftrightarrow Cr(OH)^{2+} + H^+ \quad (1)$$

$$Cr(OH)^{2+} + H_2O \leftrightarrow Cr(OH)_2^+ + H^+ \quad (2)$$

$$Cr(OH)_2^+ + H_2O \leftrightarrow Cr(OH)_3 + H^+ \quad (3)$$

An increase of the pH results in a decrease of Cr^{3+} concentration, and the species $Cr(OH)^{2+}$ becomes more abundant on the solution. Plus, the increase of the pH reduces the concentration of H^+ ions, favouring the adsorption of $Cr(OH)^{2+}$ by the negatively charged functional groups presented on the adsorbent. [13]

2.2 Methods for removing heavy metals from wastewaters

Removal of heavy metals from industrial effluents can be performed through many conventional processes, including unit operations such chemical precipitation, coagulation, activated carbon adsorption, foam flotation, ion exchange, electro-deposition, membrane operations and cementation.[14]

Among these methods, precipitation is the most used due to the economic aspects. However, the efficiency of this method can decrease due to other complexing agents in industrial effluents, originating an incomplete process and production of toxic sludge.[7] In addition, after the treatment, the effluent usually contains unacceptably total dissolved solids load.[15]

Moreover, this treatment methods have high reagent requirement, unpredictable metal ion removal, generation of toxic sludge, etc. Plus, for diluted metal ion concentrations, precipitation is ineffective.[7]

On the contrary, adsorption is a simple process and due to low-cost adsorbents, it has become the most effective method for removal of toxic pollutants from wastewaters. In fact, it is possible to ensure low cost, robustness, and versatility.[15]

In Table 2.2 are presented the main advantages and disadvantages of the most common physico-chemical processes used to treat the industrial wastewaters.

Table 2.2: Advantages and disadvantages of the main physico-chemical processes- (adapted from[16]).

Treatment method	**Advantages**	**Disadvantages**
Chemical precipitation	-Low capital cost -Simple operation -Not metal selective	-Sludge generation -Extra operational cost for sludge disposal
Coagulation/ flocculation	-Economically feasible -Bacterial inactivation capability	-Production of sludge -High consumption of chemicals and transfer of toxic compounds into solid phase
Flotation	Low operational costs -Metal selective -Low retention times -Removal of small particles	-High initial capital cost -High maintenance and operation costs
Ion-exchange	-High separation selectivity -Less sludge volume produced -Regeneration of the metal	-High investments and capital costs -Pre-treatment of effluent required -Not available for all heavy metals
Adsorption with new adsorbents	-Low-cost -Easy operating conditions -High metal-binding capacities	-Low selectivity -Production of waste products
Electrochemical treatments	-Rapid process -High separation selectivity -No consumption of chemicals	-High investment and high operation cost -Production of H_2
Membrane filtration	-Small space requirement -Low pressure -High separation selectivity	-High operational cost due to membrane fouling -Limited flow rates

2.3 Adsorption process

Adsorption corresponds to the phenomenon which in the molecules (adsorbate), present in a liquid or gaseous fluid interact at physical level with a solid surface (adsorbent), placed in vessels or packed columns. It occurs as a result of non-balanced forces on the surface of the solid that attract the molecules present in the fluid which is in contact with the adsorbent.[17]

The adsorption process is based on transport phenomena and speed of mass transference. The main in the adsorption processes is to purify and separate species present in the liquid or gaseous phase, allowing its recuperation. This process is often referred as an economic alternative in most of the cases.[18,19] The adsorption of a solute present in the fluid phase to an adsorbent, comprehends four steps, as indicated Figure 2.3:[20]

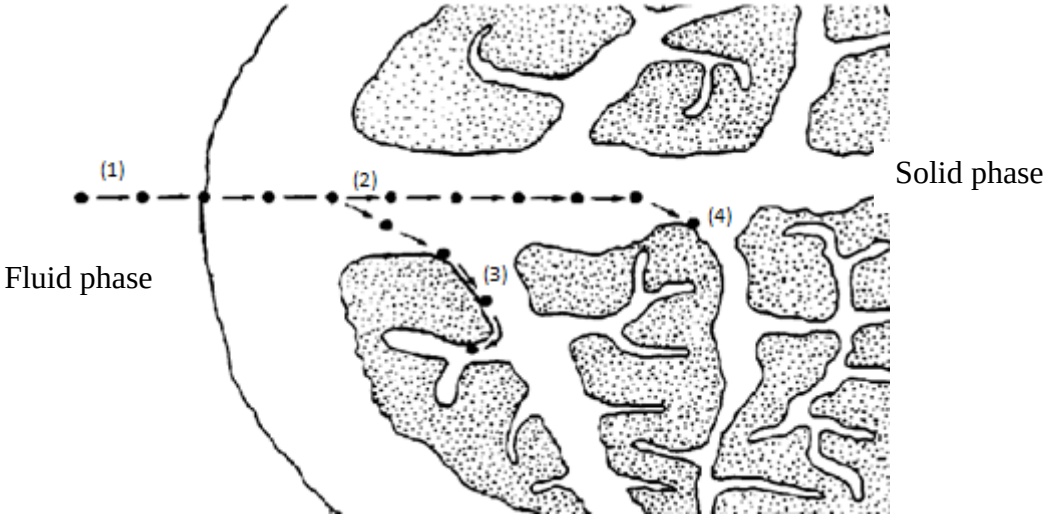

Figure 2.3: Stages of the adsorption process- (adapted from[20]).

Step 1) Occurs the transport of the species involving transport through the liquid solution to the boundary layer around the adsorbent;

Step 2) Comprehends the transport, by diffusion, of the adsorbate from the boundary layer to the entrance of the pores, denominated by external diffusion;

Step 3) Includes the transport inside the pores of the adsorbent, by molecular diffusion, through the liquid present inside of the pores and diffusion along the surface of the adsorbent;

Step 4) Occurs the binding of the adsorbate on an available adsorbent site. Depending on the saturation degree of the adsorbent, this step can be faster or slower.

The adsorption processes can be classified as chemical or physical considering the kind of forces involved:[17]

- The chemical adsorption is the process in which occurs an effective interaction between the solid surface and the adsorbed and an irreversible chemical bond is formed. From this, a formation of a single layer occur above the solid surface with a release of a considerable amount of energy is observed.
- The physical adsorption is a reversible phenomenon, where it is normally observed the deposition of one or more than one layer of adsorbate over the adsorbent surface. Van der Walls (dispersion-repulsion) forces are usually involved and the energy released is smaller compared to the chemical adsorption.

2.4 Factors affecting adsorption processes

The adsorption process may be affected by multiple factors: [19]

- **Surface area:**

Since the adsorption is based on surface interactions, the intensity of adsorption is normally proportional to the specific surface area. In other words, higher the surface areas increase the extent of adsorption. The surface area of a powdered solid adsorbent depends upon its particle size. Smaller the particle size, greater is its surface area.

- **Temperature:**

The kinetics of adsorption and equilibrium parameters are dependent on temperature. As adsorption normally releases heat (exothermic system), according to the Le-Chatelier's principle, the magnitude of adsorption should decrease with rising of temperature. It is also necessary considering that higher temperatures can damage the adsorbent and increase costs.

- **Pressure:**

The extent of adsorption is directly proportional to the pressure. So, an increase in the pressure of the system increases the extent of adsorption. At low temperature, the extent of adsorption increases rapidly with pressure. This variable has higher influence for gases.

- **pH:**

This variable determines the concentration of H^+ and OH^- groups on the solution which may interfere with the adsorbate. Usually, it is necessary to control the pH of the solution in order to control and avoid the dissociation of the active functional groups of the adsorbent, such the hydroxyl, carboxyl and phenolic groups.

- **Initial concentration:**

The adsorption process occurs due to a driving force between the adsorbent and the adsorbate. Thus, higher inlet concentrations will lead to a higher driving to adsorption. The concentration is also related to the rate of the adsorption, i.e., higher concentrations lead to higher ratios of adsorption.

- **Adsorbent dosage:**

The quantity of adsorbate removed is related to the quantity of adsorbent used. Thus, as higher dosage used, higher the removal quantity.

- **Adsorbent particle size:**

Since the adsorption process is strongly dependent on the surface area of the adsorbent, small particles are preferable because of their higher surface area. Thus, the adsorption process becomes more efficient when smaller particles are used as adsorbents.

In this way, the adsorption is a complex process that requires optimization to maximize efficiency and minimize the costs and the capital invested.

2.5 Desorption and regeneration of adsorbents

The process of adsorption in fixed bed column also includes the stage of desorption to recover the adsorbent. The desorption can be defined as the release of a substance (adsorbate) from a solid (adsorbent) either from the surface or through the surface. The desorption can occur after the saturation by changing the fluid conditions.

Since the adsorbent particles have a finite uptake capacity, the solid adsorbent may reach the saturation. At this point, the rates of adsorption and desorption are equal and equilibrium is reached. Thus, it is necessary to regenerate it or dispose of the adsorbent.[21]

Depending on the application, the adsorbent may be discarded after the usage if it has no more economic value. In the most of the cases, the disposal of the adsorbents it is not an economical solution and it is only favored when it is very difficult to regenerate and the adsorbed component as a low economic value.

The regeneration is usually carried out to recover the adsorbed substances allowing the adsorbent to be reused.[18] It can be accomplished in situ or ex situ to the adsorption vessel. Generally, after the column saturation, the adsorbent may be regenerated using suitable eluent solutions.

Taking into account that the desorption is a faster process than the adsorption, the regeneration yields smaller volumes of effluent containing concentrated adsorbate solutions.[22] This fact allows recovering the adsorbate (i.,e. heavy metals) in a simple and economical way.

Depending on the nature of the absorbent/adsorbent bonds, there are several mechanisms to accomplish desorption:[20]

- Increase of the temperature in the system;
- Change of chemical conditions, e.g. pH;
- Reduction of the partial pressure;
- Purging with an inert fluid;
- Displacement with a more strongly adsorbing species.

Figure 2.4 represents the solute concentration and temperature profiles for a porous adsorbent particle in contact with a fluid for the cases of the adsorption and desorption, respectively:

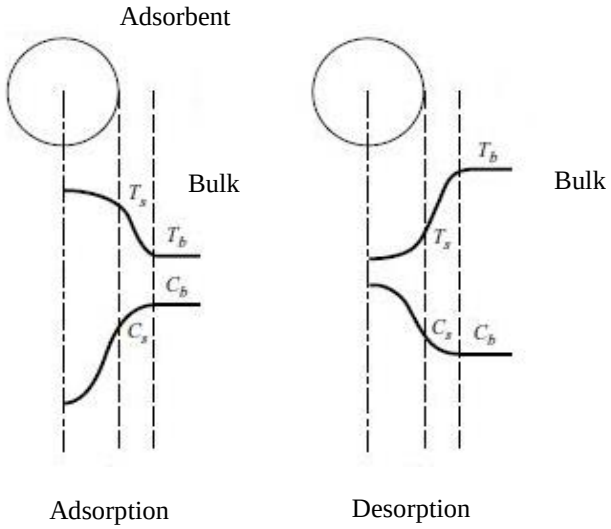

Figure 2.4: Concentration and temperature profiles in adsorption and desorption processes- (adapted from[18]).

where T_S represents the temperature on the surface of the particle and T_b the temperature in the bulk; C_s and C_b correspond to the concentration of a certain substance in the surface of the particle and in the bulk, respectively.

As it is possible to conclude, for the case of the adsorption, the concentration of a certain substance is lower inside of the adsorbent particle and higher in the bulk fluid. As the adsorption process goes on, this difference in the concentrations become lower and it reaches the equilibrium. For the case of the desorption, the opposite happens, i.e., the concentration of a certain substance inside the particle is higher and as the process runs it tends to lower until reaches the equilibrium. The temperature, in the desorption process, is higher on the bulk fluid since usually the desorption process is more efficient at higher temperatures, thus the particle surface should be at a lower temperature than the bulk fluid.

2.6 Adsorbents

2.6.1 Properties of the adsorbent

Adsorbents are usually solid particles used in the adsorption processes and their physical-chemical nature is an important factor in the adsorption, since that the capacity and the velocity of the adsorption depends on the specific surface area, porosity, specific volume of porous, distribution of the size of porous and the functional groups present on the surface of the material.[20] Typically, adsorbents have a large range of chemical forms, size of porous and different surface structure.[23]

At industrial level, a good adsorbent must:[18]

- Have high uptake capacity, to minimize the quantity of adsorbent used;
- Possess high selectivity to remove only the desired component(s);
- Have chemical and thermic stability;
- Favor the mass transport for a fast adsorption;
- Have low solubility in contact with the fluid, to preserve the quantity of adsorbent and their chemical and physical properties;
- Have high toughness and mechanic resistance to avoid the smashing and erosion;
- Allow regeneration;
- Have high open porosity;
- Do not promote undesired chemical reactions;
- Be economically viable.

2.6.2 Low-cost adsorbents

During the last decades, several studies developed technologies to remove pollutants from wastewaters and avoid disposal.

Until a few years ago, granular activated carbon (GAC) was considered the best adsorbent for wastewater treatment, due to its good capacity of adsorption. However, there is a need of replacing it due to its high cost of production and difficulties in regeneration. This economic problem has forced scientists for developing new adsorption materials.[24]

In recent years, agricultural waste materials have attracted great interest due to their basic components, including cellulose, hemicellulose, lignin, extractives, lipids, proteins, simple sugars, hydrocarbons and starch containing a variety of functional groups that facilitate adsorbate complexation.[25]

Agricultural waste materials should possess several requirements for the adsorption of metals, such as, efficient for the removal of a wide variety of heavy metals, maximum removal of specific metals, high adsorption capacity, low-processing cost, easily regenerated/disposed off after adsorption and be tolerant for a wide range of concentration of heavy metals.[26] Each one of this material has its own specific physical and chemical characteristics such as porosity, surface area, and physical strength. Adsorption capacities of the adsorbent were also found to vary, depending on their experimental conditions.

Nowadays, agricultural residues are considered economic and eco-friendly, due to their unique chemical composition and their availability in abundance being a promising option for the usage as an adsorbent for removal of heavy metals from wastewaters.[26]

Generally, lignocellulosic materials, including residues of cereals such rice bran, rice husk, coconut shells, maize corn cob, olive or cherry stones, peanut shells, grapes stalks, coffee beans, bark of the trees, sugar cane bagasse, etc, have potential metal sorption capacity, which derivate from their polymers and structure.[27] The polymers include extractives, cellulose, hemicelluloses, pectin, lignin and protein which facilitates metal complexation helping the removal of heavy metals. This type of materials is used as adsorbents for a wide range of solutes, particularly divalent metal cations.

More specifically, pine bark, for presenting all those characteristics, is shown as a material with the potential to be applied in the removal of heavy metals. However, because of its complex structure and depending on the region and the environmental conditions, the chemical composition of the pine bark may change.[28]

Despite all these differences, the pine bark is mainly constituted by lignin, polysaccharides such the cellulose and hemicellulose and a low percentage of ash.[29] Figure 2.5 shows an approximate percentage of the chemical composition of the bark of *pinus pinaster:*

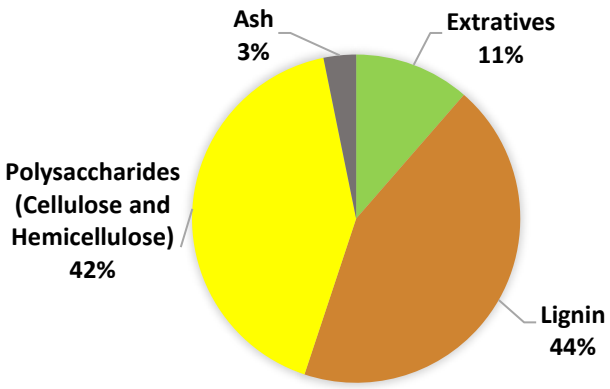

Figure 2.5: Chemical composition of the pinus pinaster bark- (adapted from[29]).

Lignin is the major component present in the pine bark and it is considered a highly branched and amorphous phenolic polymer, as it is possible to observe in Figure 2.6. It has a high surface area and contains various functional groups present in its structure, while cellulose molecules present an ordered structure composed of multiple hydroxyl, carbonyl and methoxyl groups easily accessible, making it a promising adsorbent material.[28,30]

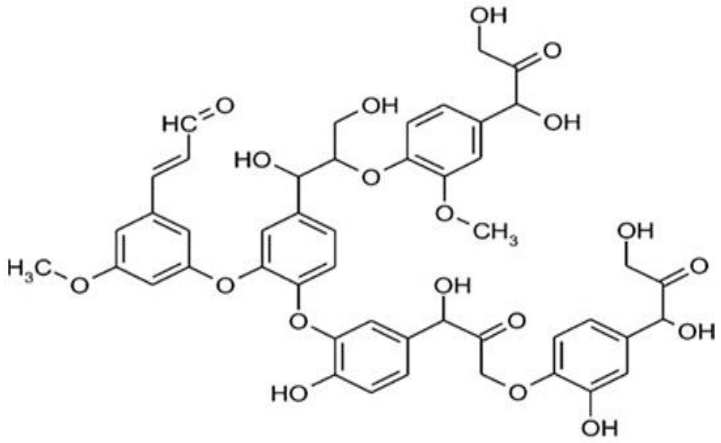

Figure 2.6: Molecular structure of lignin- (adapted from[30]).

The polysaccharides such the cellulose and hemicellulose, possess an ordered structure, as it is represented in Figure 2.7. There are four main types of cellulose, depending on their molecular structure or if it was subjected to any kind of chemical or physical treatment.[31,32] The cellulose I is the most common in nature and the cellulose II is originated by the mercerization of the cellulose I.[33,34] The cellulose III and IV are obtained also by cellulose I and II by another kind of treatments, such chemical modifications or heating. [34,35]

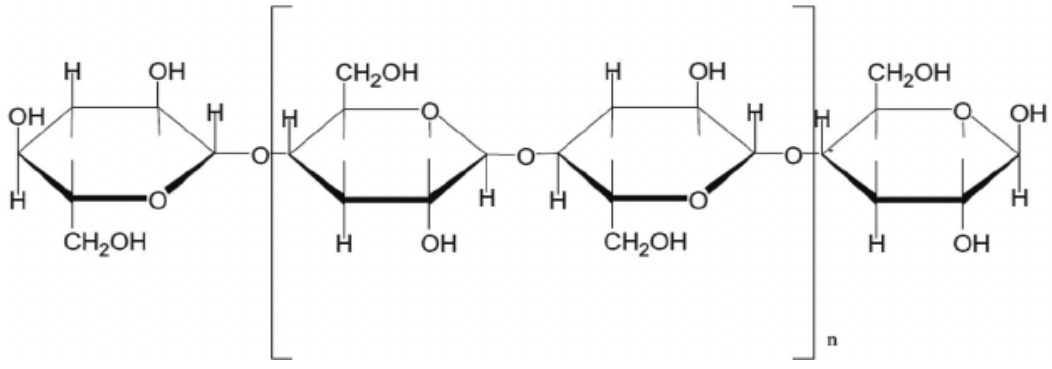

Figure 2.7: Molecular structure of cellulose- (adapted from[31]).

The hemicellulose is mainly constituted by repetitions of different monosaccharide units such the glucose and xylose with short branches of sugar units attached giving an amorphous

structure. Because of it, the hydroxyl functional groups become more accessible, and react more easily with metal ions, providing a good adsorption rate.[28,31]

The extractives, representing about 11% of the pine bark composition, are formed by a secondary metabolism of the tree, mechanical damage or attack by fungi or insects. They are constituted generally by phenols, resins, fats, and waxes, varying from species to species and their geographic location.[35]

Finally, the ash represents the inorganic constituents of the pine bark, such as Na, K, Ca, Mg, Zn and P, absorbed by the roots during the lifetime of the tree. The presence of these elements on the pine bark affects directly the pH of the material surface, with influence on the adsorption process. [28]

Despite this, the uptake capacity of the most of the lignocellulosic materials is not enough to achieve a good efficiency, their physical stability is very variable and the behavior of the cellulose, as a substrate, is highly dependent upon the crystallinity, specific surface area, and degree of polymerization.[16] Thus, raw lignocellulosic materials have been modified by various methods. These treatments increase the sorption capacity due to the number of active sites allowing an easier accessibility to hydroxyl groups, turning the lignocellulosic structure of the material more crystalline. Moreover. it also provides resistance to microbiological attack and thermal resistance[36]. Thereby metal ions adsorption take place on chemical functional groups such as carboxyl or phenolic (the chemical reactivity is a function of the high reactivity of the -OH groups present) making possible its removal from wastewaters. [37]

Considering that at pH 5 the speciation of Cr(III) metal ions is mainly $Cr(OH)^{2+}$ and the MPB has many carboxylate groups (COO^-), the binding of metal ions on the MPB surface can be represented by the Eq. (4):[38]

$$2(-COOH) + Cr(OH)^{2+} \leftrightarrow (-COO)_2Cr(OH) + 2H^+ \qquad (4)$$

where the group (-COOH) corresponds to functional groups present on the surface of the adsorbent. It is also important to work at higher values of pH since the deprotonation increase thus there are less H^+ ions to compete with $Cr(OH)^{2+}$ ions, being possible to retain a greater amount of metal ions in the adsorbent obtaining a more effective removal. However, higher values of pH above 6 can cause the precipitation of the chromium.

-Pine bark from (*Pinus pinaster*):

Nowadays, pine bark, is a sub product, especially from the industry of paper, and it is used for garden decoration or it can also be used as a bio-combustible.

As seen previously, pine bark has all the requirements for its usage as a low-cost adsorbent, specifically for the removal of heavy metals.

However, its adsorption capacity, in raw form, is not high enough to achieve good efficiencies. So, in order to achieve the best results and properties for the adsorption, the raw pine bark was subjected to an alkali treatment, known as mercerization, using an alkali solution[39]. Mercerization increases the specific surface area of the material turning hydroxyl groups more accessible, due to the change in the amorphous structure to a crystalline, providing a higher degree of substitution.[40]

Figure 2.8: Pine bark from *(Pinus pinaster).*

Pinus Pinaster is abundant in Portugal, and to valorize the bark, a low-cost adsorbent will be developed for the treatment of polluted effluents with heavy metals.

2.7 Fixed bed adsorption

Industrial processes that use adsorption as a separation process, are classified according to their operation mode. The most applied mode of operation is a column packed with adsorbent particles (fixed bed), through which the effluent will pass, adsorbing or removing one or more components present in it.[18] After a certain contact time, the column will reach saturation and will not continue to retain the components of interest. At this point, it is necessary to change the adsorbent or regenerate it.[18].

The fixed bed column in the adsorption process has several advantages in terms of assembly, cost, ease of operation, change and facility of changing the operation parameters, easy scale-up and the possibility of regenerating the adsorbent.[18,41]

The operation of fixed bed column includes a cycle of saturation or loading, the stage of desorption or regeneration and washing.[41]

2.7.1 The breakthrough concept

One of the principal requirement to design an adsorption process is the choice of the material used as adsorbent and adsorbate. It is possible to estimate the dynamic or breakthrough capacity of the column by monitoring the outflow concentration.[19] Thus, it is possible to produce a breakthrough curve. In addition to this, the height and width of the column are also important parameters to describe the system and the operation of the column.[41,42]

A characteristic scheme of a breakthrough curve is presented in Figure 2.9:

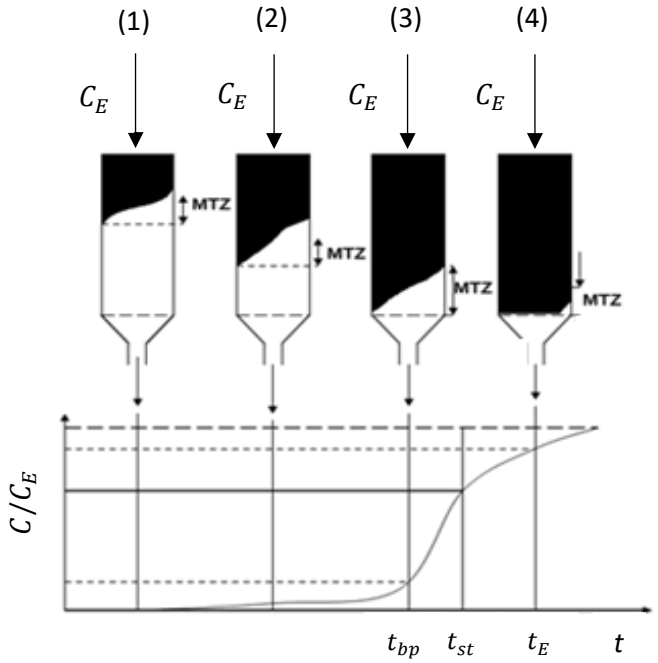

Figure 2.9: Breakthrough curve diagram where (1), (2), (3) and (4) are different moments of operation – (adapted from[42]).

Figure 2.9 shows a case where a downward flow is introduced into the column, in which the adsorbent is free of adsorbate. As the adsorbate is introduced in the column over time, close to the entrance of the column, it is formed a zone known as mass transference zone (MTZ). It moves along the column until the saturation.

In the first stage of the operation (1), the solute is adsorbed in the top of the column and the effluent of the column is free of adsorbate. As the operation continues, there will be a time that almost half of the bed is saturated and a saturated zone is formed (black area), however, the concentration of the adsorbate in the effluent is zero (2). When the MTZ reach the bottom of the column the breakthrough point (t_{bp}) is attained (3). Usually, the breakthrough point is considered as 1% of the inlet concentration in the column.[41] Generally, the breakthrough time

(t_{bp}) decreases with the increase of the particle size, higher concentrations of the solute in the effluent, higher values of pH of the influent, high flow rates and low bed depths.[43]

After the system reaches this point, the concentration of the solute on the effluent increases rapidly and the column can still operate until the MTZ achieve the exit of the bed and the concentration of the effluent reaches 95% of the inlet concentration (4). This point is denominated the exhaustion time (t_E). From this point on, the concentration of the effluent increases slowly until equalize the inlet concentration of the solution. At this moment, the adsorption process is finished. [41]

Another important parameter is the stoichiometric time (t_{st}), that is defined as the time where the area above the breakthrough curve is divided into two equal areas, which correspond to the 50% of the bed saturation. Through the mass balance at the column, it is possible to obtain:

$$QC_E t_{st} = \varepsilon V C_E + (1-\varepsilon)\varepsilon_p V C_E \Leftrightarrow t_{st} = \tau\,(1+\xi) \tag{5}$$

where Q is the flow rate (mL/min), $C_E(mg/L)$ represents the feed concentration, ε the bed porosity, $V(m^3)$ the bed volume, ε_p the porosity of the particles, the $\tau(min)$ is defined as residence time, calculated by Eq.(6) and ξ corresponds to the capacity factor calculated by Eq.(7):

$$\tau = \frac{\varepsilon V}{Q} \tag{6}$$

$$\xi = \frac{(1-\varepsilon)}{\varepsilon}\frac{q}{C_E} + \frac{(1-\varepsilon)}{\varepsilon}\varepsilon_p \tag{7}$$

where q (mg/g) represents the adsorption capacity.

The useful capacity of the bed, defined as the instant where the solute is detected in the effluent of the column, corresponds to the breakthrough point and it can be represented as the S_1 area, observed in the Figure 2.10:

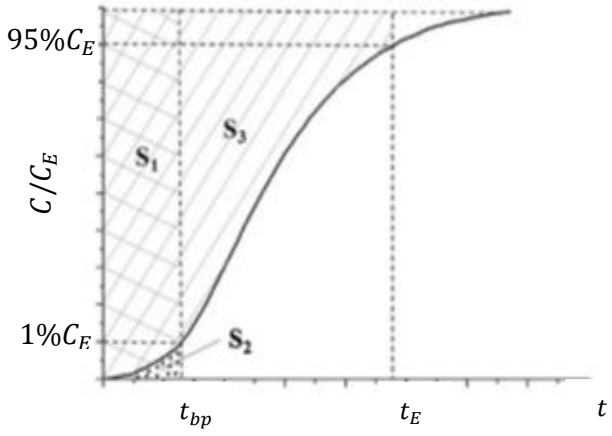

Figure 2.10: Typical representation of a breakthrough curve.

The stoichiometric time, t_{st} , is defined as the time taken for the actual capacity to be used and it is also the point that breaks the MTZ into equal areas, and can be calculated as:

$$t_{st} = \int_0^{t_\infty} \left(1 - \frac{C}{C_E}\right) dt \tag{8}$$

where C (mg/L) is the concentration of the effluent during the operating period.

The saturation bed fraction (FLS) can be calculated as:

$$FLS = \frac{\int_0^{t_{bp}} \left(1 - \frac{C}{C_E}\right) dt}{\int_0^{\infty} \left(1 - \frac{C}{C_E}\right) dt} = \frac{S_1}{S_1 + S_3} \tag{9}$$

and represents the relationship between the total mass of chromium adsorbed in the column until the breakthrough point and the mass of chromium introduced into the column through the feed. It can also be determined as a function of the S_1 area divided by the total area above the breakthrough curve until the exhaustion time, S_3, as represented in the Figure 2.10.

The amount of metal ions, $m_{total}(mg)$ feed to the column can be calculated as:

$$m_{total} = Q \times C_E \times t_f \tag{10}$$

Through the breakthrough curve is possible to calculate the total of mass not adsorbed, in mg, of the metal ion, which corresponds to the area under it. For a given flow rate and feed concentration the total not adsorbed quantity, m_{na} (mg), can be determined by the following expression:

$$m_{na} = Q \times \int_0^{t_f} C \, dt \tag{11}$$

The quantity of metal adsorbed at the equilibrium or the adsorption capacity, q (mg metal/ g adsorbent) can be calculated from the combination of the previous equations, divided by the amount of adsorbent introduced, $m_{ads}(g)$:

$$q = \frac{m_{total} - m_{na}}{m_{ads}} \tag{12}$$

The shape and time of the breakthrough curve are important parameters that need to be taken into account for assessing the dynamic behavior of the fixed bed column. The inlet concentration, the bed depth, the flow rate, the particle size of the adsorbent and the adsorption equilibrium relationships are determinant factors that need to be taken into consideration to describe this system.[19]

For the cases of plug flow operation, the diffusional resistance to mass transfer in the column is null and if the adsorption process was infinitely fast, the system response obtained

would be a step set up in t=t_{st} as illustrated in Figure 2.11. However, in a real situation it, does not happen so the diffusional mass transfer resistance must be considered.

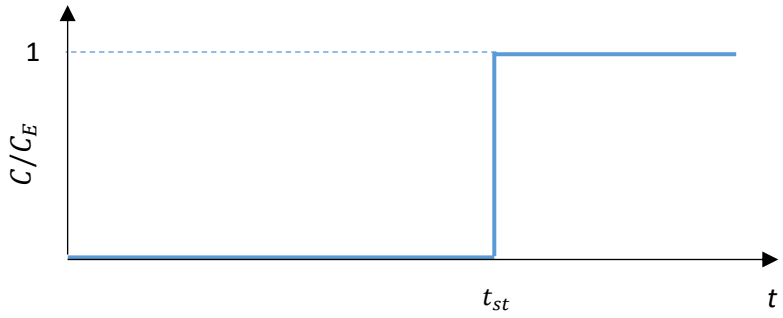

Figure 2.11: Breakthrough curve for plug flow in the bed.

The factors that affect the breakthrough curve can be divided in thermodynamic, kinetic and hydrodynamics. The thermodynamic factors are the ones that determine the distribution of the solute between the fluid and the solid phase, which includes the inlet concentration, porosity of the bed and of the particle, capacity of the adsorption, temperature, and pressure. These relationships are described in the adsorption isotherms and were determinate in the previous work[44,45].

The kinetic factors can be distinguished in four stages of mass transfer: the transference from the solution to the film surrounding the particle, the external diffusion (through the film), the internal diffusion (through the porous structure) and adsorption over the interparticle surface.[45] These characteristics are also related with the hydrodynamics of the system that determines the diffusion mechanisms. There are several diffusional mechanisms in the macropores including the molecular diffusion, Knudsen diffusion and surface diffusion. The diffusion on the micro pores is associated with interactions of potential field and steric effects.[19,45]

2.7.2 Mathematical models of fixed bed adsorption

A mathematical model is a possible way for describing a system in terms of the relations between operational variables and parameters. In other words, a mathematical model tries to describe the phenomenon occurring in a system to gain prediction capacity.[46] This kind of models are used to analyze the behavior of complex systems in situations usually difficult to observe.[47]

Generally, the mathematical modelling is a technique based on mathematical equations to describe a real system with the aim of predicting his behavior under certain conditions.

The project and design of the unit operations, such the fixed bed columns, is usually accomplished through the use of mathematical models.[46-48] The development of mathematical models and computer simulation are an important tool because it allows the transfer of technology from the laboratory to industrial scale.

In this point of view, mathematical models show many useful aspects as the possibility of add or reject certain hypothesis related to complex phenomena, show unexpected responses or predict the behavior of a system under conditions that were not tested yet. However, the closer the model to reality, the more complex it will be, involving a higher number of parameters resulting in a greater difficulty to obtain the data from the model and its interpretation.[49]

The main goal of mathematical modelling to describe a phenomenon is the possibility of reducing the costs associated with real experiences, increase the speed of data collection and the development of control systems.

Some aspects are necessary for validation and evaluation of a mathematical model, which:[47]

- Should be able to describe the behavior of the of the real system;
- Should be able to support theories or hypotheses that explain the behavior;
- Must be able to predict the behavior, namely the effects of changes in the variables of the system or in its mode of operation;
- Must be able to respond to changes of variables with the same sensitivity presented by the experimental model.[50]

Mass balance:

Thus, the construction of a mathematical model to simulate a fixed bed column is not an easy task. The model must take into account the nonlinearity in adsorption equilibrium isotherms, interference effects due to solute competition by adsorbent sites, the resistance of mass transfer between the fluid phase and the solid phase and the hydrodynamic dispersion phenomena.

For modelling the adsorption of Cr(III) in a fixed-bed, the following assumptions were made:[51]

- At the beginning of the operation, the material inserted in the column (MPB) is assumed to be pure, with zero concentration of Cr(II) in the whole column;
- At time t = 0 min the feeding of the column starts from the top to bottom of it (descending);
- All sorption parameters remain constant along the column (axial dispersion coefficient, mass transfer coefficient, liquid and solid phase, as well as kinetic constants);

- Bed packing and porosity are uniforms throughout the column;
- The flow rate is constant and invariant with the column position;
- Hydraulic effects such as flow preferences and 'clogging' are not considered;
- Mixing in the feed reservoir is perfect;
- The temperature is constant in the feed and the bed (thermal effects are not important).

It is important to note that at any point in the column, the solute concentration in the liquid phase is a function of time and position along the column because the system operates in a non-stationary state relative to solute concentrations in the liquid phase.

Thus, the model includes the mass balances in the fluid phase, ion-exchange equilibrium isotherms and intraparticular mass transfer governed by a linear driving force (LDF).

The distribution of a component in the fluid and solid phases is obtained through the mass balance. Neglecting the radial dispersion along the column, there are only two independent variables: time (t) and length of the column (z). The transient mass balance includes the term of axial dispersion, convection flow term, accumulation in the fluid phase and the adsorption process on the adsorbent particles[52]. Thus, considering a volume element of the bed [$A \times \Delta z$] in an adsorption column, the mass balance is represented by the following equation:

$$\begin{bmatrix} Flux\ of\ mass\ that \\ enters\ in\ a\ certain \\ element\ of\ volume \end{bmatrix} - \begin{bmatrix} Flux\ of\ mass\ that \\ exits\ a\ certain \\ element\ of\ volume \end{bmatrix} = \begin{bmatrix} Accumulation\ of \\ mass\ in\ the \\ volume\ element \end{bmatrix} \quad (13)$$

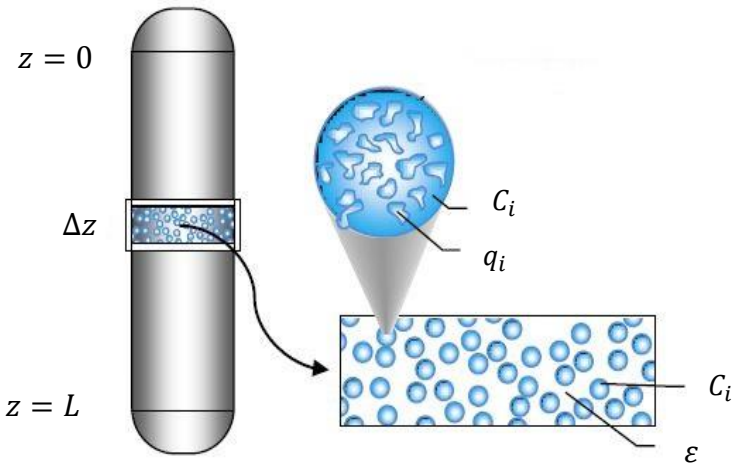

Figure 2.12: Volume of control of the adsorption unit in fixed bed column- (adapted from [52]).

The flux of mass that enters in a certain volume element, N_z, is given by Eq. (14) and the flux of mass that exits from a certain volume element, $N_{z+\Delta z}$, is given by the Eq. (15):

$$N_z = \varepsilon A_s \left(u_0 C - D_{ax} \frac{\partial C}{\partial z}\right)\Big|_{z,t} \tag{14}$$

$$N_{z+\Delta z} = \varepsilon A_s \left(u_0 C - D_{ax} \frac{\partial C}{\partial z}\right)\Big|_{z+\Delta z,\, t} \tag{15}$$

The term of accumulation of the mass in the element of volume is given by the following expression:

$$A_s \Delta z \left(\varepsilon \frac{\partial C}{\partial t} + \rho_p f_h \frac{\partial q}{\partial t}\right)\Big|_{z,t} \tag{16}$$

Considering that the interstitial velocity and axial dispersion coefficient are constants along the column and replacing Eqs. (14), (15) and (16) on the (13), the final mass balance can be presented by:

$$\frac{\partial C(z,t)}{\partial t} + u_i \frac{\partial C(z,t)}{\partial z} + \frac{(1-\varepsilon)}{\varepsilon} \rho_p f_h \frac{\partial \langle q(z,t)\rangle}{\partial t} - D_{ax} \frac{\partial^2 C(z,t)}{\partial^2 z} = 0 \tag{17}$$

where D_{ax} is the axial dispersion coefficient (m^2/s) , u_i the interstitial velocity (m/s), ε the bed porosity, z (m) the axial position, $C(mg/L)$ the concentration of the species Cr(III) in the bulk fluid phase, $\langle q \rangle$ $(mol/kg_{adsorbent})$ the average adsorbed phase concentration in the adsorbent particles, ρ_p the density of the adsorbent(kg/m^3) and f_h its the humidity factor.

Eq. (16) is a partial differential equation of second order. So, the first term represents the accumulation of the component in the fluid phase, the second term represents the mass transfer in the column due to the convective effects, the third term represents the accumulation of the component in the solid phase and the fourth term represents the mass transfer due to the effects of axial dispersion.[46]

The term of the axial dispersion (Peclet number) may be described by Eq. (18) and the Reynolds number by Eq. (19):

$$\frac{u_o d_p}{D_{ax}} = (0.2 + 0.011 Re^{0.48}) \tag{18}$$

$$Re = \frac{u_o \rho_f d_p}{\eta} \tag{19}$$

in which the term $u_o(m/s)$ is the superficial velocity, d_p (m) the average particle diameter, ρ_f the density (kg/m^3) and η $(Pa.s)$ the viscosity of the solution, respectively.

Adsorption equilibrium isotherm:

The equilibrium isotherms adsorption for the chromium, represents the adsorption capacity, $q^*(mg/g)$ as a function of the adsorbate liquid concentration at the equilibrium, $C_e(mg/L)$, was adjusted by the Langmuir model:

$$q^*(z,t) = \frac{q_m K_L C_e}{1 + K_L C_e} \tag{20}$$

where q_m (mg/g) is the maximum adsorptive capacity and K_L a parameter which relates to the adsorption energy:

$$K_L = K_L^{\infty} exp\left(\frac{(-\Delta H)}{RT}\right) \tag{21}$$

The Langmuir isotherm is a theoretical model and assumes that the adsorption occurs in specific sites of the specific surface, without interactions between adsorbed molecules and the adsorption process is limited to a monolayer coverage.[53]

Another common equation to describe the equilibrium is the Freundlich isotherm:

$$q^* = K_f \times C_e^{1/n} \tag{22}$$

where K_f ($mg^{1-(1/n)}L^{1/n}/g$) is the Freundlich isotherm constant and n is an isotherm constant that represents the adsorption intensity.

Figure 2.13 shows the equilibrium isotherms and the experimental data, performed in batch mode, in previous works[44], for the Cr(III) adsorption:

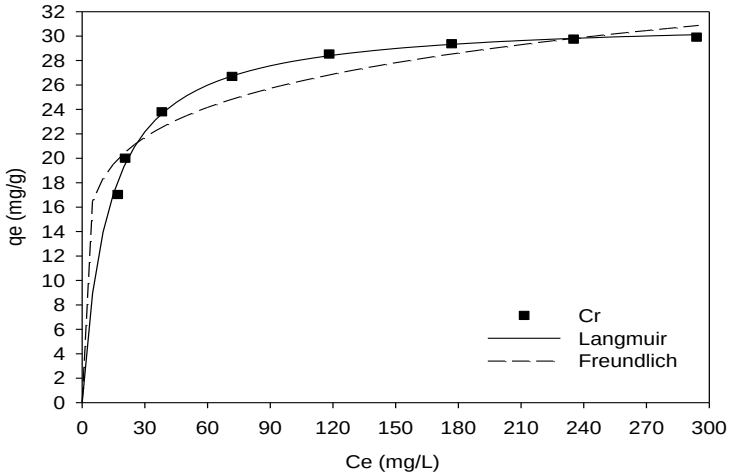

Figure 2.13: Equilibrium isotherms (initial concentration of Cr(III) = 500 mg/L, temperature = 25℃ and pH 5)- (adapted from[44]).

For the present work, the Langmuir isotherm will be used to express the equilibrium, since this model has a better adjustment to the experimental data.

Intraparticle mass transfer:

In cases where the geometry of the adsorbent particle is not well defined, the use of the linear driving force model (LDF) appears as an alternative for modeling these processes. The LDF approximation, introduced by Glueckauf (1955)[54], admits that the mean adsorbed phase concentration rate is proportional to the difference between the adsorbed phase concentration in equilibrium with the bulk and the mean adsorbed phase concentration, as indicated in Eq. (23):[53]

$$\frac{\partial\langle q(z,t)\rangle}{\partial t} = k_{LDF}[q^*(z,t) - \big(q(z,t)\big)] \tag{23}$$

where k_{LDF} is the LDF kinetic constant and $q^*(z,t)$ is the adsorbed phase concentration of the species in equilibrium with the bulk concentration.

The LDF model assumes:[54]

- Equilibrium between concentrations on bulk fluid and on particle surface;
- The mass transfer kinetics occurs infinitely fast, meaning that exists an instantaneous equilibrium between the pore fluid concentration and the adsorbed concentration.

The k_{LDF} used in the model was estimated by Eq. (24), based on the equivalence of LDF models for homogeneous and porous particles:

$$k_{LDF} = \frac{\Omega D_{pe}}{r_p^2 \rho f_h(\frac{dq^*}{dC})} \tag{24}$$

where Ω is the LDF factor, which is equal to 15 for spherical particles, $D_{pe}(m^2/min)$ represents the effective pore diffusivity, r_p (m) the radius of the particle of the adsorbent and $(\frac{dq^*}{dC})$ the slope of the equilibrium data, obtained by the batch experiments.[44]

D_{pe} was calculated by the following expression:

$$D_{pe} = \frac{\varepsilon_p D_m}{\tau} \tag{25}$$

where D_m is the molecular diffusivity of the solute in water, τ the tortuosity of the adsorbent and ε_p its porosity. The molecular diffusivity expressed in (m^2/s), for metal ions, can be estimated by the Nernst equation (26) and depends on the equivalent ionic conductance of the metal in solution, λ , and on the valence of the ion, Z:[55]

$$D_m = 2.661 \times 10^{-11} \frac{\lambda}{|Z|} \tag{26}$$

Boundary and initial conditions:

The Danckwerts boundary conditions were considered for solving the mass balance equations:

-for z=0 : $D_{ax}\frac{\partial C(z,t)}{\partial z} = u_i(C(0,t) - C_E)$ (27)

-for z= L : $\frac{\partial C(z,t)}{\partial z} = 0$ (28)

where C_E represents the feed composition and L is length of the bed.

The following initial conditions were applied, which simulates the start-up of the fixed-bed column:

- for t=0, $C(z,0) = 0$, $q(z,0) = 0$ (29)

The numerical solution of the partial differential equations (PDE), that describes the mass transfer in the fluid phase, was obtained by using the Finite Difference technique, that converted PDE into a set of ordinary differential equations (ODE).[53]

A script was implemented in MATLAB to solve those equations coupled with equations that describe the intraparticle mass transfer.

3. STATE OF THE ART

3.1 Heavy metal removal in fixed bed column

Adsorption process by dynamic methods, more specific by column systems has shown to be advantageous over the batch type operations because the rate of adsorption is highly dependent on the concentration of the solute in the effluent that need be treated.

For column operation, the adsorbents are continuously in contact with a fresh solution, which means that the concentration in the solution in contact with the adsorbent, present in the column is relatively constant. On the other hand, for batch adsorption, the concentration of solute in contact with the adsorbent continuously decreases, causing a decrease in the effectiveness.[26]

The adsorption process in fixed bed columns is the most used among continuous systems due to their advantages. However, the disadvantage of this method is that it takes a long operation time to attain equilibrium, thus a large solution volume is necessary to saturate the column[56]. Recently, some studies were made using fixed bed columns to treat wastewaters and industrial effluents.

Agricultural residues have shown interesting adsorption properties, namely low-cost. Despite their good properties and potential to be a future solution for the wastewater treatment containing heavy metals the investigation in this field is recent.

In order to compare the adsorption capacities to metal cations of agricultural waste materials, Table 3.1 was constructed.

As it possible to observe, the studies were performed with pH in the range 3.5 to 5.8, which means that all the experiments were carried out in an acid environment, favoring the presence of divalent and trivalent metal cations. The adsorption capacity of agricultural waste materials is in the range of 1.7 to 105.98 mg/g but for Cr(III) the capacities were in the range 4.96 to 68.12 mg/g. Some adsorbents were subjected to chemical treatment. However, sometimes the adsorption capacity did not have a significant increase.

Considering the operational conditions, it is possible to conclude that for the most cases, the higher values of adsorption capacity are achieved when it is used higher initial pollutant concentration, keeping the other parameters constant. Moreover, higher adsorption capacity was obtained for lower flow rates. For the case of the *Orange (citrus cinesis)* and *Pinus sylvestris* sawdust, the bed depth does not have an influence on adsorption capacity.

Table 3.1: Column studies on adsorption of heavy metals.

			Operational conditions					Results				Ref.
Adsorbate	**Adsorbent**	**Model**	**C_E mg/L)**	**pH**	**H (cm)**	**D (cm)**	**Q (mL/min)**	**q (mg/g)**	**t_{bp} (min)**	**t_{st} (min)**	**t_E (min)**	
Cr(III)	Hemp fibers (Alizarin S)	Thomas and Yoon–Nelson	13	5.8	7	1.5	2.1	6.89	110	-	300	[57]
		Thomas and Yoon–Nelson	26.14	5.8	7	1.5	2.0	10.78	80	-	220	[57]
	Olive stone	BDST	10	4	13.4	1.5	2	4.96	55	-	-	[58]
		BDST	25	4	13.4	1.5	2	7.89	13	-	-	[58]
		BDST	50	4	13.4	1.5	2	12.25	2.5	-	-	[58]
		BDST	75	4	13.4	1.5	2	11.72	-	-	-	[58]
		BDST	100	4	13.4	1.5	2	12.09	-	-	-	[58]
	Sargassum filipêndula ($CaCl_2$ 0,2M)	MB_LDF	16.5-100	3	30.6	2.8	6	33.51	-	-	-	[59]
	Orange (citrus cinesis)	BDST	20	4	25.5	2.2	8.5	12.48	1025	-	2922	[22]
		BDST	20	4	34	2.2	8.5	12.48	1523	-	3426	[22]
	Biomass of Seaweed *Sargassum*	MB_LDF	54.1	3.5	30.6	2.8	2	66.56	-	-	-	[13]
		MB_LDF	52.5	3.5	30.6	2.8	6	60.32	-	-	-	[13]
		MB_LDF	52.5	3.5	30.6	2.8	8	68.12	-	-	-	[13]
Co(II)	Natural hemp fibers	Thomas model	25	4.5-5	7	1.5	-	15.44	-	215.9	-	[60]
		Thomas model	50	4.5-5	7	1.5	-	18.01	-	126.1	-	[60]
		MB_LDF	33.09	3.5	30.6	2.8	6	81.47	-	-	-	[61]
Cu(II)	Marine alga Sargassum	MB_LDF	66.2	3.5	30.6	2.8	6	92.91	-	-	-	[24]
		MB_LDF	102.16	3.5	30.6	2.8	6	105.98	-	-	-	[24]
		MB_LDF	202.4	3.5	30.6	2.8	6	104.39	-	-	-	[24]
Pb(II)	*Pinus sylvestris* sawdust	BDST	10	5.5	6.5	1.5	2.51	5.7	443	-	-	[62]
		BDST	10	5.5	8.5	1.5	2.51	6.4	648	-	-	[62]
		BDST	10	5.5	13.0	1.5	2.51	6.6	1030	-	-	[62]
		BDST	3	5.5	13.0	1.5	10	1.7	220	-	-	[62]
		BDST	5	5.5	13.0	1.5	10	1.6	121	-	-	[62]
		BDST	10	5.5	13.0	1.5	10	2.2	85	-	-	[62]
Ni(II)	Waste of tea	Thomas	100	4	30	2	5	11.13	-	-	-	[63]
		Thomas	100	4	30	2	10	10.57	-	-	-	[63]
		Thomas	100	4	30	2	20	7.48	-	-	-	[63]
		Thomas	50	4	30	2	10	7.31	-	-	-	[63]
		Thomas	75	4	30	2	10	9.45	-	-	-	[63]
		Thomas	200	4	30	2	10	11.17	-	-	-	[63]

MB_LDF: Mass balance equations applied to an element of volume of the column in the liquid phase and in the solid phase plus LDF model; BDST: Bed depth service time model

Higher initial concentration of pollutant leads to lower breakthrough time (t_{bp}), while higher bed depths (more quantity of adsorbent on the column). (t_{bp}). For example, in the study of *Orange (citrus cinesis)*, the column needs more time to reach the exhaustion for the higher bed depth.

The adsorption capacity of the agricultural residues, generally, found to be satisfactory and considering the advantages of this type of materials, and the promising results of our teamwork, it was decided to investigate the performance of the modified Pinus bark for the removal of Cr(III) from the wastewater using a fixed-bed column.

During the study, operational parameters, such the initial concentration of pollutant, the bed depth and the superficial velocity, will be changed in order to optimize them, with the final goal of maximizing the removal of Cr(III).

3.2 Mathematical models for fixed bed adsorption

Currently, a variety of mathematical models have been used to describe and predict the breakthrough curves of a column adsorption system. However, there is still a lack of a comprehensive review of these models.

The optimization of the design and the operation conditions of the fixed bed adsorption system is an important topic to focus on. Thus, a reliable model should be able to predict accurately the breakthrough curve and evaluate the effect of each parameter involved in the adsorption process.[56] As consequence, to simplify the fixed bed adsorption, by making appropriate assumptions based on a certain system, several models were proposed based on different simplifications.

Despite several models has been developed to estimate the behavior of the system, the oldest models remain in use, not only because of their good prediction of dynamic adsorption but also because they allowed determining important operational parameters.[46]

In a process with n variables, the optimization of them can be done by keeping (n-1) variables fixed and compare the effect of different values in the remaining variable on the predicted breakthrough curves by the model. However, the main limitation of these models, and therefore, the optimization of the process becomes difficult because of the complexity and time-consuming computation simulation[46].

Some models, assume that the rate of intraparticle diffusion is described by Fick's law. Table 3.2 shows the main general dynamic models used for that purpose:[46]

Table 3.2: General dynamic models for column adsorption process.

Model	Equation	Ref.
Pore diffusion model (PDM)	$\varepsilon\frac{\partial C}{\partial t}+\frac{\partial q}{\partial t}=\frac{\rho D_{ep}}{r^2}\frac{\partial}{\partial r^2}\left(r^2\frac{\partial q}{\partial r}\right)$	48
Homogeneous surface diffusion model (HSDM)	$\varepsilon\frac{\partial C}{\partial t}+\rho\frac{\partial q}{\partial t}=\frac{D_s}{r^2}\frac{\partial}{\partial r^2}\left(r^2\frac{\partial q}{\partial r}\right)$	64
Pore and surface diffusion model (PSDM)	$\varepsilon\frac{\partial C}{\partial t}+\rho\frac{\partial q}{\partial t}=\frac{D_s}{r^2}\frac{\partial}{\partial r^2}\left(r^2\frac{\partial q}{\partial r}\right)+\frac{\rho D_{ep}}{r^2}\frac{\partial}{\partial r^2}\left(r^2\frac{\partial q}{\partial r}\right)$	65

In Table 3.3 are present another two general dynamic models, however more complex, that explains with more detail the diffusional phenomena's, also based on Fick's law. This models, like the PDM, HSDM, and PSDM, describes the dynamic behaviour of the adsorption process, in fixed-bed column, but in this cases some assumptions were made in order to describe more efficiently the interactions between the adsorbent and the ions, present in the fluid phase, inside the porous particles of the adsorbent.

Table 3.3: More detailed general dynamic models for column adsorption studies.

Modification	Assumption	Equation	Ref.
Macropore diffusion and micropore diffusion	Postulating each adsorbent pellet is composed of a core and outer region with macropore	-Diffusion equation of macropore region: $\frac{\partial q}{\partial t}=\frac{1}{r^2}\frac{\partial}{\partial r^2}\left((D_e)_{Ma}\,r^2\frac{\partial q}{\partial r}\right)$, $r_c < r < r_p$; -Diffusion equation of micropore region: $\frac{\partial q}{\partial t}=\frac{1}{r^2}\frac{\partial}{\partial r^2}\left((D_e)_{mi}\,r^2\frac{\partial q}{\partial r}\right)$, $0 < r < r_c$; -Mass conservation at the interface: $(D_e)_{Ma}\left(\frac{\partial q}{\partial r}\right)_{r\to r_c^+}=(D_e)_{mi}\left(\frac{\partial q}{\partial r}\right)_{r\to r_c^-}$	64
Shrinking core theory model	This model used to describe the intrapellet adsorption is controlled by pore diffusion, supposing adsorption firstly occurs at the outer region of the adsorbent, then the mass transfer zone moves inward together with the extending of the saturated outer region and shrinking of the unloaded core.	-The mass transfer flux at the solid-liquid phase interface: $J=4\pi r_p^2 k_f(C-C_e)$; -Diffusion in the pore of adsorbent (Fick's law): $J=\frac{4\pi C_e r_p r_c D_{ep}}{r_p-r_c}$; -The velocity of mass transfer zone: $\frac{dr_c}{dt}=-\frac{J}{4\pi r_c^2\rho q_e}$; -The mean concentration of the adsorbed solute: $\overline{q=q_e\left[1-\left({}^{r_c}/_{r_p}\right)^3\right]}$	66

For solving equations shown in Table 3.2 and 3.3 it is necessary to deal with specific mathematical difficulties. The equations showed in Table 3.4 have been proposed to overcome some of these issues. For example, the wave propagation theory, the constant pattern theory, and LDF model can be used together with general dynamic models, indicated in Table 3.1 and 3.2 to globally obtain a solution.

In Table 3.4 are represented a list of the most used models in this category:

Table 3.4: Additional models to express adsorbate-adsorbent interactions.

Model	**Equation**	**Ref**
Wave propagation theory	-Velocity of the 'concentration wave: $$u_c = \frac{u_i}{1 + \frac{\rho}{\varepsilon}\left(\frac{dq}{dC}\right)}$$ where, $\left(\frac{dq}{dC}\right)$ is calculated by the corresponding isotherm $q_e = f(C_e)$	67
Constant pattern theory	-Overall mass transfer equation: $$\rho\left(\frac{dq}{dC}\right) = \varepsilon K_L a(C - C_e)$$	68
Linear driving force (LDF)	-Mass transfer coefficient to represent the intrapellet diffusion rate: $$\frac{dq}{dt} = k_e(q_s - q_a)$$	54

To modify the intraparticle diffusion models, empirical models were developed, based on different simplifying hypotheses, making them less complex and less time-consuming. Although being models constructed based on empirical relationships, such the Thomas model, the Clark model, the BDST model and the Yoon-Nelson model, they show a good prediction and they are usually used to describe the behavior of the breakthrough curve, as represented in Table 3.5.

In addition, for obtain the dynamic solution, the choice of the isotherm will directly affect the results of the mathematic model. Even though researchers have developed various isotherm models, it is difficult to find one that fits well in all the cases. Due to the fact of each adsorbent has his own structure and characteristic interactions between different ions, isotherms can present diverse shapes. So, is the best way to determine isotherms is by conducting experiments.

In the present work, a mathematical general dynamic model that includes a mass balance, an adsorption equilibrium isotherm and the LDF model to describe the mass transfer was chosen to predict the dynamic behavior of the fixed bed adsorption.

Table 3.5: Empirical models for column adsorption studies.

Model	Equation	Ref
Thomas model	$\frac{C_t}{C_0} = \frac{1}{1 + exp\left(\frac{k_{Th}}{Q(q_0 x - C_0 V e_{ff})}\right)}$	66
Clark model	-Mass conservation equation: $\rho J = -u_i \varepsilon \frac{\partial C}{\partial z} - \varepsilon \frac{\partial C}{\partial t}$	69
Bohart-Adams model and bed depth service time (BDST) model	$ln\left(\frac{C_F}{C} - 1\right) = ln\left[exp\left(k_B q_m \frac{H}{u}\right)\right] - k_B C_F t$	70
Yoon-Nelson model	$ln\frac{C}{C_F - C} = K_{YN} t - t_{1/2} K_{YN}$	71

Although the LDF model is not the most complete model to explain the behavior intraparticular mass transfer, it can significantly reduce the computational time showing an acceptable precision.

4. MATERIALS AND METHODS

4.1 Materials

4.1.1 Adsorbate

In this study, the Cr(III) used were of analytical grade and purchased from Alfa Aesar. The solution of chromium(III) with a concentration of 100, 200 and 300 mg/L were prepared by dissolving chromium nitrate nonahydrated, $Cr(NO_3)_3{\cdot}9H_2O$, with ultrapure water. The final pH of the solution was 5, adjusted with a solution of 1M NaOH. For the regeneration tests, two regenerative agents were used: N,N-Bis(carboxymethyl)-DL-alanine trisodium salt (N,N-Bis) from Sigma-Aldrich and nitric acid (HNO_3) from Fluka.

4.1.2 Adsorbent

The adsorbent used in this study was pine bark, species *Pinus pinaster*, collected in North of Portugal, sub-region of Pinhal Litoral in the Tâmega's valley.[44]

In the first stage, the pine bark was washed with distilled water to remove the dirt, fungus and dust. After washing, it was dried in the oven at 90 ºC for 24 h to remove water possible. The oven-dried bark was crushed in a Reischt MUHLER, model 5657 HAAN and sieved using JULABO model SW-21C to desired mesh size (0.088mm-0.149mm) for being treated.

4.1.2.1 Adsorbent modification

-Mercerization Treatment

Then, the washed pine bark was put in contact with a NaOH solution 10% w/w, at 25ºC, during 16 h with constant stirring, with the goal of increasing the adsorption capacity of the material.

To lower the pH of the modified pine bark, it was washed and filtered with tap water until a neutral and constant pH. In the final stage, ultrapure water was used to remove any other contaminants such calcium or chloride that could be present in tap water. At the end, the material was dried in an oven at 90 ºC for 24 h and stored in a desiccator.

The main properties are shown in Table 4.1:

Table 4.1: Physical properties of MPB.

ρ (Kg/m^3)	f_H	d_p (mm)	Surface area (m^2/g)	Average pore diameter (Å)	Pore volume (cm^3/g)
320-360	0.95	$3.48\text{x}10^{-2}$ - $1.97\text{x}10^{-1}$	8.74	166.40	0.04

4.2 Experimental methods

4.2.1 Column experiment

The fixed-bed column studies were performed using a laboratory-scale glass column D-46539 Dinslaken of 15 mm internal diameter and 120 mm height. A peristaltic bomb Minipuls3-Gilson, was used to feed the column with the inlet solution at a predefined flow rate.

The column allows to adjust the height of the fixed-bed and was in the vertical position. There were two filters, one on the top and other on the bottom, to avoid any movement of the adsorbent in the column.

The feed of the column was introduced on the top of it as showed in Figure 4.1. First, a low flow rate of ultrapure water was introduced to ensure the bed becomes completely wet, to prevent a preferential flow. After that, the flow rate was set to the desired value and the chromium solution was introduced. Samples were collected at the exit of the column to analyze the concentration of the metal.

In the saturation experiments, samples were collected until the outlet concentration reached the inlet concentration. All the experiments were carried out at room temperature (20 ± 2°C).

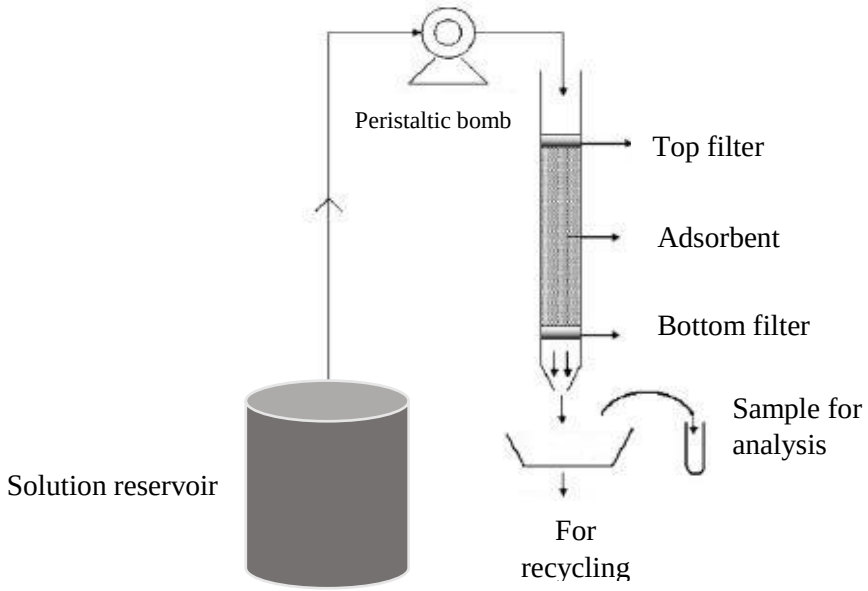

Figure 4.1: Fixed-bed column apparels used in experiments.

For the case of the regeneration test, the same procedure was used, but the solution percolated in the column, previously saturated, was the regenerating agent. The experiments were conducted at 25°C and 50°C, by heating the solution before its feeding to the column.

4.3 Analytical techniques

4.3.1 Dynamic Light Scattering (DLS)

The particle size distribution of the adsorbent was measured by Dynamic Light Scattering (DLS) from Malvern.

The adsorbent was suspended with ultrapure water. Then, the particles were analyzed through this equipment, which measures the intensity of the scattered light. The fluctuations, caused by the Brownian movements, contain the information about the particle size distribution and can be analyzed as a function of time, enabling the evaluation of particle size.[72]

Figure A.1 showed in Appendix A, depicts particle distribution in the range of 0.034824 to 0.196671mm with an average diameter of 0.099046mm.

4.3.2 Moisture of the adsorbent

The moisture content was measured in duplicate, using a crucible washed and dried for 12h. Then, about 1 g of material was weighed and was placed in an oven during 24 h at 105℃ and the dried mass was registered.

To calculate the moisture of the material, Eq. (30) was used:

$$H(\%) = \frac{m_i - m_d}{m_i} \times 100 \tag{30}$$

where $m_i\ (g)$ is the initial weight and $m_d\ (g)$ is the weight at the end of 24 h of drying.

4.3.3 Bed porosity analysis

The bed porosity was measured by filling a certain height of the column with kerosene and the mass introduced was registered. Then, the column was filled with the particles of adsorbent filled with kerosene and the weight registered. The difference between the mass of the column before and after filled with the solid can be transformed into volume, which corresponds to the void spaces.

The porosity of the fixed-bed was calculated by Eq. (31):

$$\varepsilon = \frac{V_{voids}}{V_{total}} \tag{31}$$

Two experiences were done (29.19% and 32.09%) and the average value corresponds to 30.64%.

4.3.4 Elemental Analysis by Energy-Dispersive X-Ray Fluorescence (EDXRF)

EDXRF is an analytical technique which allows determining the elemental chemical composition of the sample, providing both quantitative and qualitative information.[73]

This technique can be classified as an atomic emission method and thus can measure the wavelength and intensity of light emitted by energized atoms in the sample, irradiated by a primary X-ray beam. Since each element, emits a characteristic radiation, it allows determining the type of elements present in the sample.

The equipment used was the Rigaku's ART with a range of 0 to 1000 mg/L.

4.4 Experimental planning

-Design of experiments:

Generally, there are many possible factors that can affect a certain system, some may be critical and have more relevance than others which may have a minor effect or none on a response of the system. It is intended to reduce the number of factors, usually to a small set (2-5), in order to understand what are the most relevant factors and how they affect the dynamics of the system, giving them the major focus.[74]

In this case, the methodology of Design of Experiments was used with the aim of identify which factors have the bigger relevance on the fixed-bed adsorption process and also perceive the interaction between them.

The experiments were designed based on Box-Benken Design (BBD) and on Table 4.2 are showed the inputs for the (BBD):

Table 4.2: Parameters and factor levels.

Factor	**Level**		
	Low (-1)	**Central (0)**	**High (+1)**
Superficial velocity (cm/s)	9.62×10^{-2}	14.43×10^{-2}	19.24×10^{-2}
Bed-depth (cm)	2.5	5.0	7.5

5. RESULTS AND DISCUSSION

5.1 Experimental and calculated breakthrough curves

The objective of the study was to determine optimal conditions of two operating variables (fluid superficial velocity and bed depth) of the Cr(III) sorption process in fixed bed by applying a Box-Benken Design. A set of 9 (3^n) experiments were performed according to the conditions given in Table 5.1. The performance of the process should be evaluated by comparing the amount of the solute adsorbed and leaving the column in the effluent, as well as the time required for the entire operation. Therefore, it is desirable to minimize the difference, $\Delta t_{ads} = (t_E - t_{bp})$, reducing thus the unused portion of the column, and on the other hand to maximize the saturation bed fraction (FLS).

Table 5.2: Factorial design of the experiences performed.

Run	Bed depth (cm)	Superficial velocity (cm/s)x10^2
1	2.5	9.62 (10)*
2	2.5	14.43 (15)
3	2.5	19.24 (20)
4	5	9.62 (10)
5	5	14.43 (15)
6	5	19.24 (20)
7	7.5	9.62 (10)
8	7.5	14.43 (15)
9	7.5	19.24 ((20)

*****The values in brackets correspond to the flow rate, in mL/min, calculated as: $\boldsymbol{Q = u_o\ (\pi\ d^2/4)}$.

5.1.1 Effect of fluid superficial velocity on breakthrough curves

Since the cross sectional area of the column is constant and uniform implicates that the linear flow rate (superficial velocity) of the fluid through the packed bed it is directly proportional to the overall volumetric flow rate percolated into the column. The fluid superficial was used as independent variable in the optimization process because its value usually is kept constant in the case of the scale-up of fixed-bed adsorbers.[62]

The effect of superficial velocity on the Cr(III) adsorption by MPB was studied by varying the flow rate through the bed depth from 10 to 15 and 20 mL/min and keeping constant the inlet solute concentration (C_E =100 mg/L) and the bed depth. Figure 5.1 shows the plots of the chromium concentration in the effluent at outlet column versus the contact time when the superficial velocity varied nearly from 0.1 to 0.2 cm/s for bed heights of 2.5, 5 and 7.5 cm.

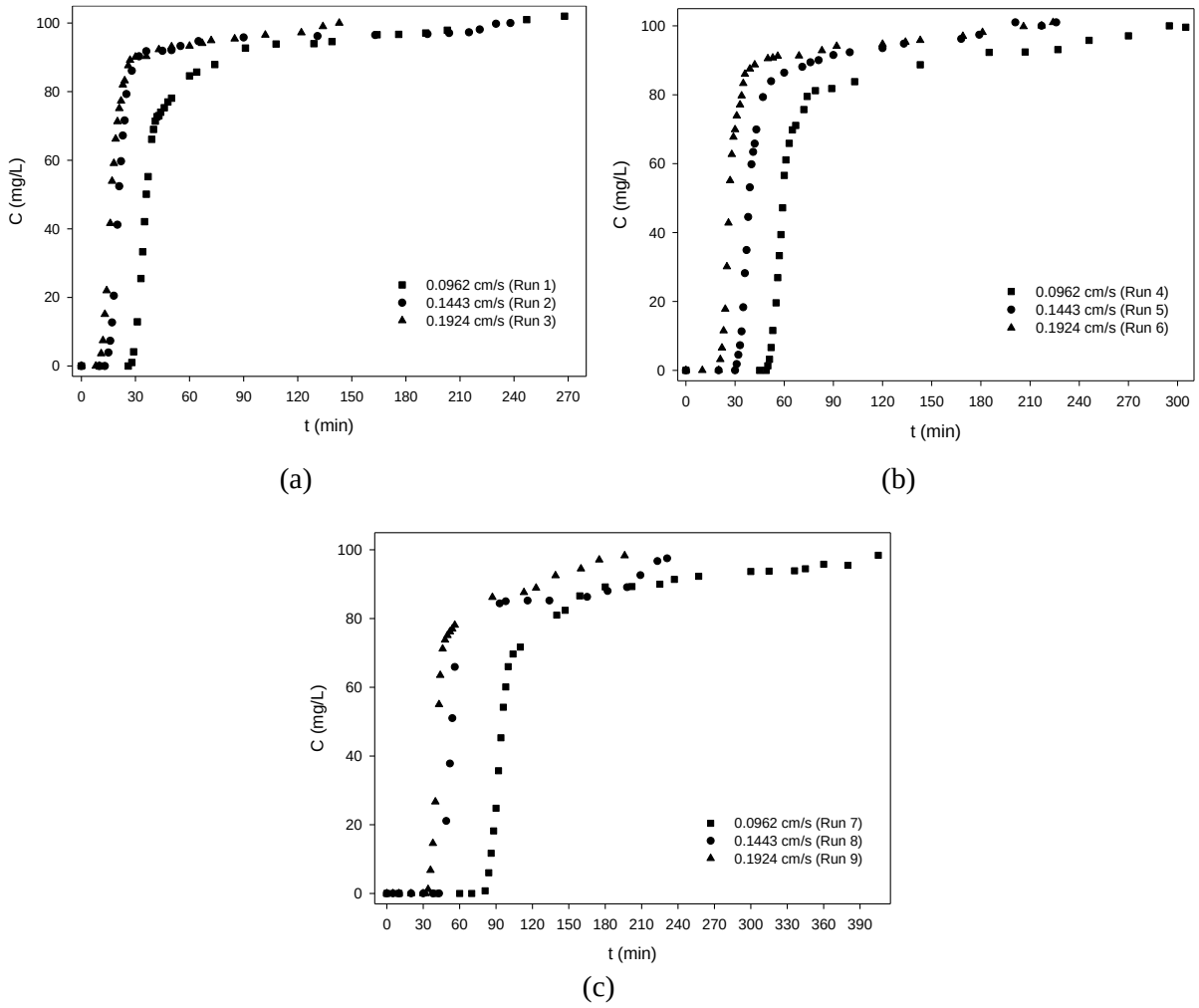

Figure 5.1: Experimental breakthrough curves of Cr(III) adsorption in MPB using different superficial velocities: (a) H = 2.5 cm, (b) H = 5.0 cm and (c) H = 7.5 cm.

For all the experiments, it can be observed that the breakthrough curve becomes steeper and the adsorbent gets saturated early as the superficial velocity increases. This may be explained due to the fact of at higher flow rates, thus, higher superficial velocities, the contact time between the metal ions and the adsorbent decreases leading to lower efficiency of mass transfer of Cr(III) ions from solution to the adsorbent. As it is possible to observe in Fig. 5.1, for each different bed depth used, the breakthrough curve emerged faster with the increase of the superficial velocity.

The conditions of the experimental design and the values of relevant parameters calculated from the breakthrough curves are summarized in Table 5.2. In this Table, it can be seen that as the superficial velocity is increased, the breakthrough time (t_{bp}) and the exhaustion time (t_E) were found to decrease to all the experiments. This can be explained because, at higher flow rates, the adsorption rate, controlled by the intraparticle diffusion, tends to decrease such as the residence time (τ).[75]

Table 5.2: Experimental conditions and calculated parameters to assess the process performance.

Run	$u_o \times 10^2$ (cm/s)	H (cm)	C_E (mg/L)	t_{bp} (min)	t_E (min)	t_{st} (min)	q (mg/g)	FLS	τ (min)	Δt_{ads} (min)	ξ
1	9.62	2.5	99.8	27.61	141.63	48.57	30.49	0.38	0.14	114.01	358.29
2	14.43	2.5	99.3	13.51	62.39	31.43	29.45	0.40	0.09	48.89	347.78
3	19.24	2.5	99.3	10.27	68.47	24.79	30.96	0.40	0.07	58.19	365.69
4	9.62	5.0	99.5	49.75	237.03	80.85	30.24	0.61	0.27	187.28	297.90
5	14.43	5.0	101	30.55	161.75	51.87	29.54	0.58	0.18	131.19	286.62
6	19.24	5.0	100	20.31	127.00	37.12	27.91	0.53	0.14	106.69	273.42
7	9.62	7.5	98.2	81.12	287.41	123.97	30.36	0.62	0.41	206.29	304.76
8	14.43	7.5	97	43.26	207.59	73.43	26.64	0.55	0.27	164.31	270.65
9	19.24	7.5	98.8	33.62	153.28	56.99	28.09	0.57	0.20	119.66	280.14

The values of the stoichiometric time, (t_{st}), decrease as the superficial velocity increases as shown in Table 5.2. Since the t_{st} splits the breakthrough curve into two equal areas, it is expected that the stoichiometric time takes lower values for the cases when the column reaches the saturation earlier, which corresponds, for each bed depth, to the higher superficial velocity used.

As the adsorption rate is mainly controlled by intra-particulate diffusion, the adsorption capacity (q) tends to increase as the superficial velocity decreases because the residence time is longer, thus the intra-particular diffusion becomes more effective. Therefore, the Cr(III) metal ions have more time to diffuse to the inside of the adsorbent particles, making possible to reach higher values of adsorption capacities. For example, for a bed depth of 5 cm and velocity of 9.62 $x10^{-2}$ cm/s, the adsorption capacity (q) is 30.24 mg/g while for the superficial velocities of 14.43$x10^{-2}$ cm/s and 19.24$x10^{-2}$ cm/s the values q estimated are of 29.54 and 27.91 mg/g, respectively.

It is now worth analyzing the effect of the superficial velocity on the two response variables (Δt_{ads} and FLS) that characterize the process performance. As already mentioned previously, the breakthrough and the exhaustion times tend to decrease as the superficial velocity increases, consequently $\Delta t_{ads} = (t_E - t_{bp})$ decreases. However, the saturated bed fraction (FLS) is little affected by the velocity change.

Regarding the capacity factor (**ξ**), this parameter takes the highest value in the Run 3, corresponding to approximately 366. This was expected since this parameter is dependent on the stoichiometric time and residence time, and adsorption capacity. So, it is expected that the capacity factor assumes higher values for the experiments where higher adsorption capacities and stoichiometric times where achieved and also for lower residence times.

5.1.2 Effect of bed depth on breakthrough curves

Another parameter that influences the breakthrough curve in adsorption processes is the bed depth. This factor is one of the most influential on the breakthrough point that determines the amount adsorbed in a fixed-bed column. Figure 5.3 shows the breakthrough curves obtained for Cr(III) ion adsorption for different bed depths (2.5, 5 and 7.5 cm), keeping constant the superficial velocity and inlet Cr(III) concentration.

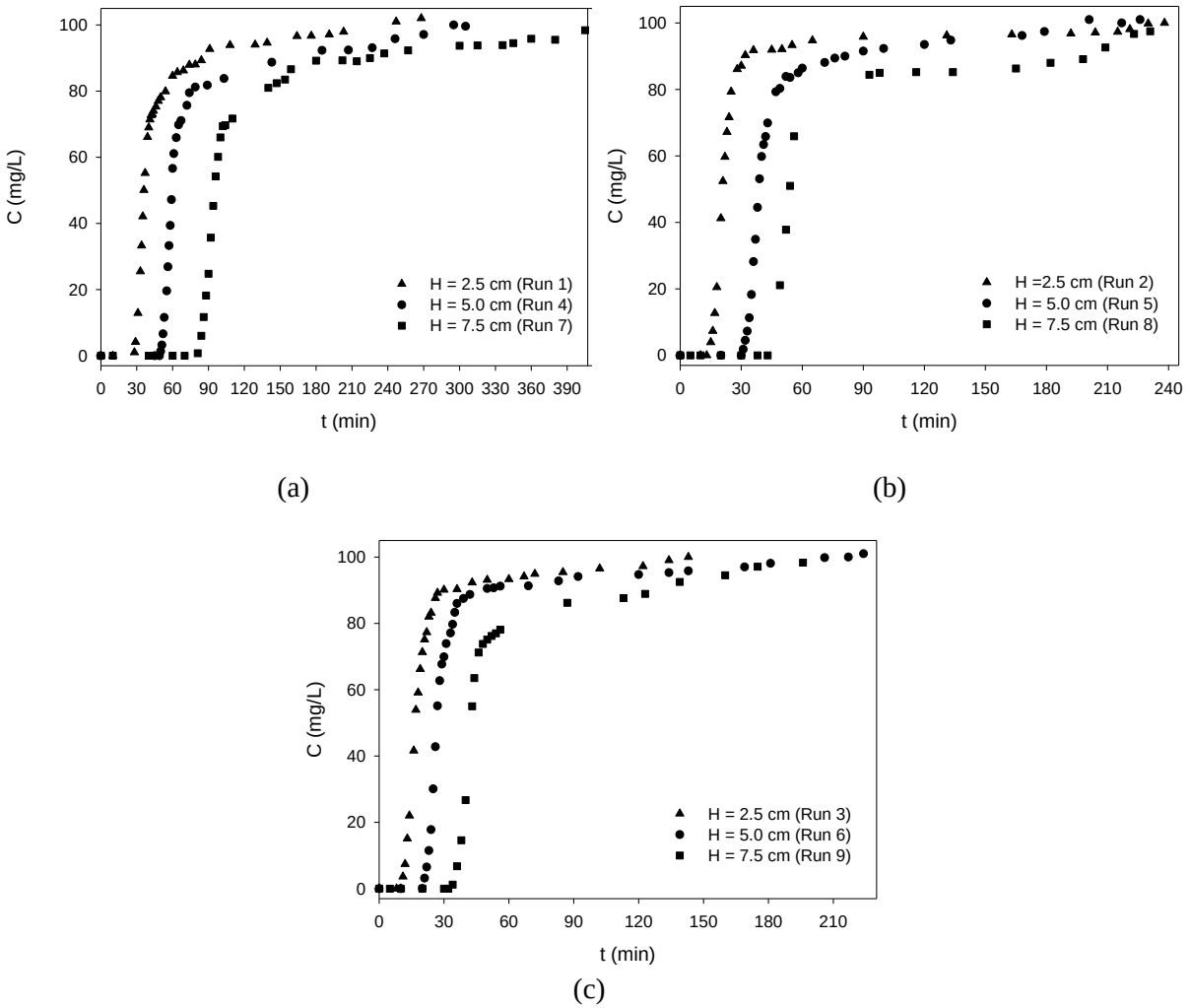

Figure 5.2: Experimental breakthrough curves of Cr(III) adsorption in MPB using different bed depths (a) u_o=9.62x10^{-2} cm/s, (b) u_o=14.43x10^{-2} cm/s, and (c) u_o=19.24x10^{-2} cm/s.

Contrarily to the effect of the superficial velocity, increasing the bed depth the breakthrough time also increase resulting in a higher operating time to take the column to the exhaustion point. For example, as shown in Table 5.2, the t_{bp} increases from 27.6 to 81.1 min in the case of the superficial velocity of 9.62x10^{-2} cm/s, when the bed depth varied from 2.5 to 7.5 cm. This is due to the fact of as much quantity of adsorbent introduced in the column, more binding

sites are available for sorption resulting in a broadened mass transference zone (MTZ). For smaller bed depths, the axial dispersion phenomena predominate in the mass transfer process leading to a reduction of the diffusivity of the metal ions. Consequently, the metal ions do not have enough time to diffuse into the adsorbent, leaving the column earlier.[62]

The contact time (τ) between the solution and adsorbent is higher when the bed depth increases. This results in a higher adsorption capacity because the metal ions had more time to diffuse deeper inside the adsorbent particles, which provide greater surface area. Therefore, higher amounts of Cr(III) ions are removed from the solution, whose values are obtained from the area above the breakthrough curves.

The adsorption capacity (q) values shown in Table 5.2 exhibit non-significant changes with variation of bed height. Comparing the q values, where superficial velocity was kept constant, it is possible to observe that the adsorption capacity remained practically unalterable. This can also be expected because since the adsorption capacity does not depend on the quantity of material used being an intrinsic characteristic of the adsorbent. For all the experiments, the maximum adsorption capacity was determined as approximately 31 mg/g, concerning to the Run 3, which is similar to that found in the batch studies, $q_m = 31.41$ mg/g.[44]

Concerning to the stoichiometric time (t_{st}), this parameter increases with the increase of the bed depth, as can be seen in Table 5.2. The higher value of t_{st} (≈124 min) was obtained for the operating conditions ($u_o = 9.62 \times 10^{-2}$ cm/s and H =7.5 cm) that lead to a higher fraction of used bed (Run 7), in which FLS = 0.62. The response variable FLS takes higher values for higher bed depths since the saturated bed fraction (FLS) is quite influenced by the breakpoint time (t_{bp}). Moreover, the variable ($t_E - t_{bp}$) tends also to increase as the bed depth increases, at constant superficial velocity.

In order to maximize FLS, observing the results of the experiments carried on, it was possible to conclude that the optimum operating point corresponds to the conditions of Run 7, where the bed depth and superficial velocity are 7.5 cm and 9.62×10^{-2} cm/s, respectively.

5.1.3 Effect of feed concentration on breakthrough curves

The performance of the adsorption of Cr(III) ions in fixed-bed column was also tested varying the feed concentration of chromium. These experiments were performed maintaining constant the optimal conditions identified from the experimental design results ($u_o = 9.62 \times 10^{-2}$ cm/s and H = 7.5 cm) and with inlet solute concentrations of 98.2, 202 and 302 mg/L.

In Figure 5.3 are displayed the results of the effect of the variation of the inlet concentration of Cr(III) on the breakthrough curves. It can be seen that as the inlet concentration (C_E)

increases the saturation curve becomes steeper. In addition, the adsorbent reaches the saturation faster and the breakthrough time decreases with the increase of the feed concentration. Contrarily, for lower inlet concentrations, the breakthrough curve appears later and consequently, the adsorbent takes more time to saturate.

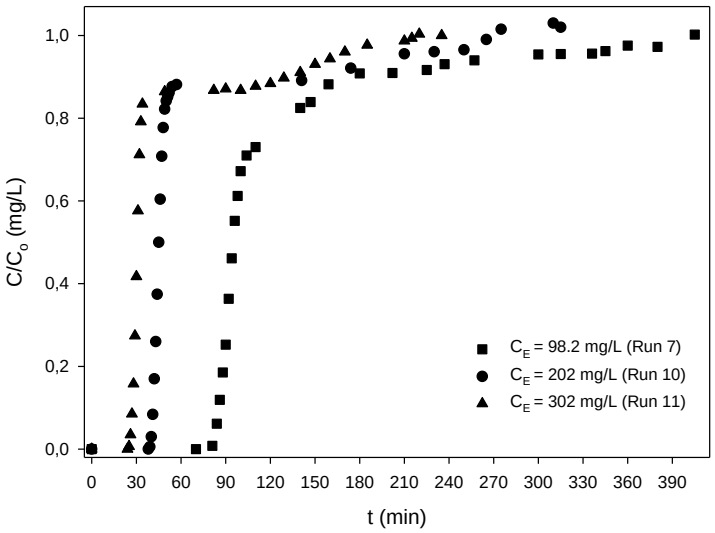

Figure 5.3: Effect of the feed concentration on the experimental breakthrough curve of Cr(III) adsorption in MPB using different feed concentrations.

As Table 5.3 shows, the breakthrough time (t_{bp}), the exhaustion time (t_E) and the stoichiometric time (t_{st}) assumes lower values when higher feed concentrations are used. For example, a reduction of 62.1% in t_{st} was verified when C_E was tripled. This may be explained by the fact that the available binding sites of the adsorbent become saturated more quickly at high metal concentration entering into the column. Under these conditions, there is a higher concentration gradient which leads to a faster solute transport due to an increase diffusional coefficient or mass transfer coefficient.[57] Therefore, it can be concluded that the mass transference zone (MTZ) becomes smaller due to an increase of metal loading rate. At lower solute concentrations, meaning lower concentration gradient, the driving force is not sufficient to enhance mass transfer and the MTZ is enlarged. This can also be observed by the values of Δt_{ads} presented in Table 5.3. The smaller the value of this parameter is, the smaller is the mass transfer zone. In other words, the lower this value, steeper the breakthrough curve is, i.e. closer of ideal saturation conditions.

Table 5.3: Experimental conditions and calculated parameters to assess the process performance.

Run	$u_o \times 10^2$ (cm/s)	H (cm)	C_E (mg/L)	t_{bp} (min)	t_E (min)	t_{st} (min)	q (mg/g)	FLS	τ (min)	Δt_{ads} (min)	ξ
7	9.62	7.5	98.2	81.12	287.41	123.97	30.36	0.62	0.41	206.29	304.76
10	9.62	7.5	202	39.19	204.34	62.06	31.26	0.61	0.41	165.16	165.16
11	9.62	7.5	302	25.12	163.8	46.94	35.35	0.50	0.41	138.68	138.68

Regarding the parameter $\Delta t_{ads} = (t_E - t_{bp})$, it was found to be the lowest when a concentration of 302 mg/L is used because the adsorbent molecules are subjected to a higher driving force, leading to a faster saturation of the column, thus the time between the breakthrough point and the exhaustion point is significantly reduced.

Analysing Table 5.3, it is also possible to observe that a small increase (≈ 17%) in the adsorption capacity (q) is noticed when C_E varied from 98.2 to 302 mg/L, which is consistent with the trend of the equilibrium isotherm obtained for the system modified pine bark/Cr(III). The maximum adsorption capacity was achieved for C_E = 302 mg/L, which corresponds to 35.35 mg/g. The capacity factor (ξ) that depends on the ratio q/C_E tends to increase as the inlet concentration decreases affecting directly the fraction of saturated bed (FLS). FLS was approximately doubled when a one-third reduction in C_E is verified. This means that operating at lower metal feed concentrations allows to use larger column capacity and maximize the sorption yield.

5.2 Comparison of the simulation model with the experimental results

To analyze the robustness and precision of the model, which comprises a set of equations defined in section 2.7.2, experimental breakthrough curves are shown together in the same plot with ones obtained from the simulations using the model.

In order to solve the model equations, it was necessary to use the information displayed in Table 5.4, namely the properties of the adsorbent (MPB), the bed characteristics, equilibrium parameters and mass transfer parameters. The values considered for the density and diameter of the particles had to undergo minor adjustments inside the ranges shown in Table 5.4 due to the physical heterogeneous nature of the adsorbent material.

Table 5.4: Properties and parameter values used in the simulation.

Adsorbent (MPB)	Bed properties	Equilibrium parameters	Mass transfer parameters
ρ (Kg/m^3) = 320-360	L (mm) = 25-75	q_{max} (mg/g) = 31.41	D_{pe} (cm^2/min) = 1.314x10^{-4}
f_H = 0.95	D (mm) = 15	K_L (L/mg) = 0.08	D_{ax} (cm^2/min) = 2.86x10^{-2} – 5.67x10^{-2}
d_p (mm) = 5.5x10^{-2} - 9.9x10^{-2}	ε = 0.306	dq/dC = 0.98	

In Figure 5.4 are illustrated the obtained experimental data, for each case of study, and ones obtained from the simulations.

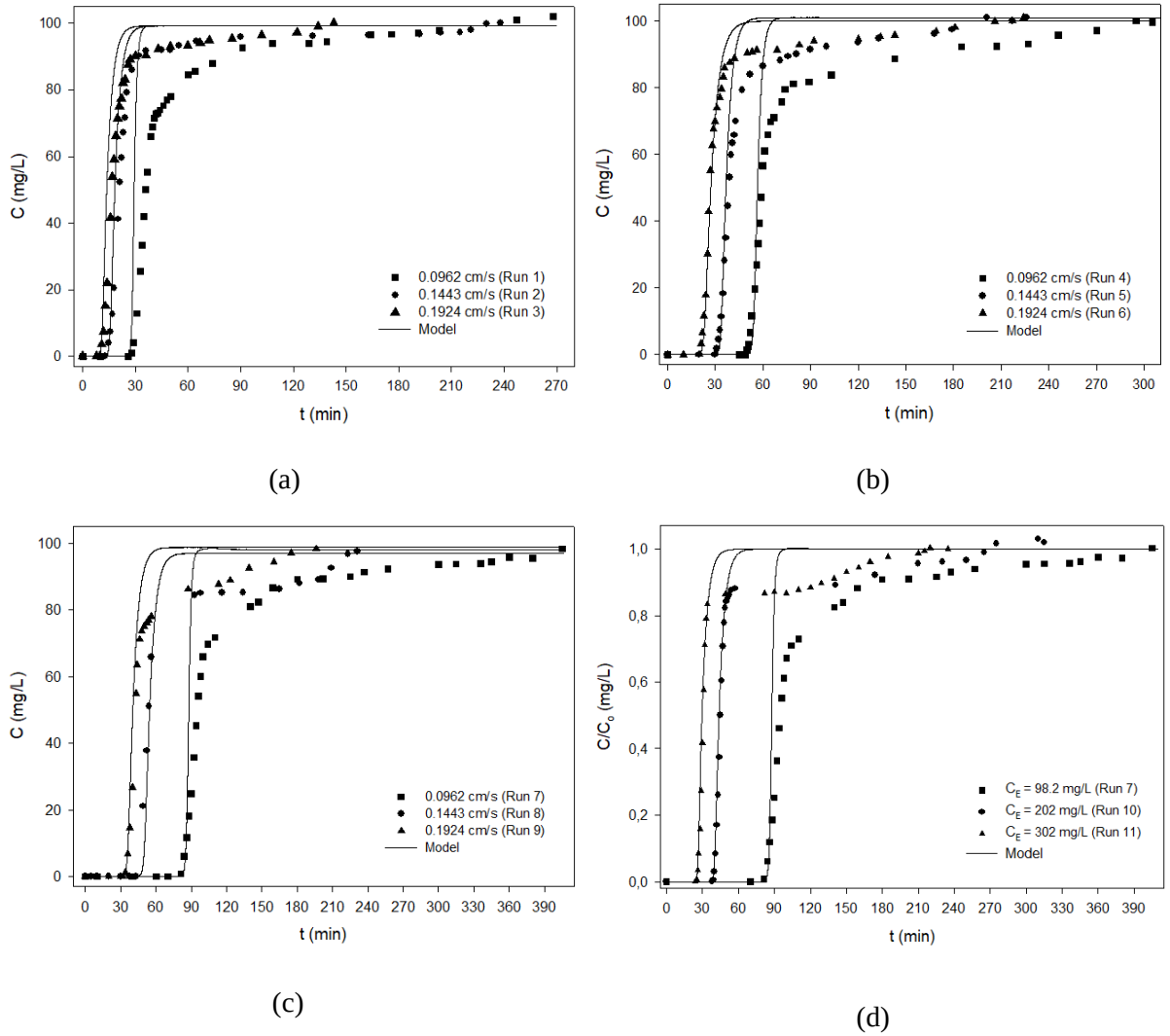

Figure 5.4: Experimental and simulated breakthrough curves of Cr(III) adsorption (a) H = 2.5 cm, (b) H = 5.0 cm, (c) H = 7.5 cm and (d) Effect of feed concentration on breakthrough curves (98,2, 202 and 302 mg/L).

The comparison of the experimental and calculated breakthrough curves shows that the model satisfactorily fits the experimental data corresponding to the dynamics of the sorption process of Cr(III) using a column packed with chemically modified pine. However, as it is possible to observe for all the cases, the model does not describe accurately the behavior of the system when the column is close to the saturation. This may be related to the intraparticular mass diffusion behavior. Since the LDF equation used is a simplified model that does not allow interpret accurately the concentration profile inside the particle due to intraparticular mass transfer resistance.

To surpass this problem, a more complete model should be considered incorporating differential equations to describe more precisely the mass transfer inside the adsorbent in order to get a more accurate description of the reality. However, this model will become more complex requiring advance numerical methods to solve. Even so, it is possible to conclude that the best predictions of the model were achieved for the cases in which lower bed depths (2.5 and 5 cm) and higher superficial velocity were used, as well as higher metal inlet concentration.

5.3 Statistical treatment (DOE)

As already mentioned above, the response variables Δt_{ads} and FLS are important parameters for the optimization of the sorption process in a fixed bed. A set of experiments were performed accordingly to a Box-Benken-design factorial design where the factors considered were the superficial velocity and the bed height (Table 4.1).

A first analysis of the experimental breakthrough curves by using the software *Statistica7*, considering as the dependent variable the saturated bed fraction (FLS), was carried out. From the software, it was possible to obtain the Pareto chart, shown in Figure 5.5.

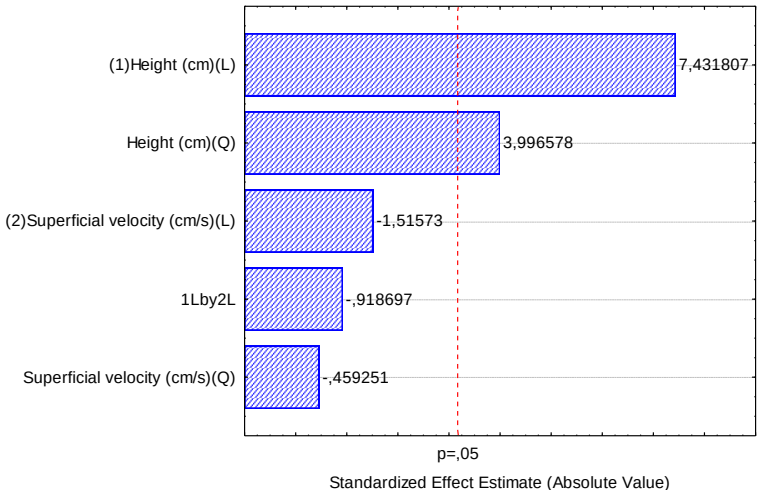

Figure 5.5: Pareto chart of the factors affecting FLS.

It allows to assess the extent and significance of the effects of the factors on FLS at the 95% confidence level. As it can be observed, the bed height and the superficial velocity are significant variables for the column utilization efficiency, where the height is the variable that most influences the response variable FLS.

A predictive model relating the FLS to the independent variables (H and u_o) was generated by the software and is given by Eq. (32). The comparison between the experimental and model predicted values can be seen in Fig. 5.6 and Table 5.5. It is possible to conclude that the values that exhibit higher deviation from ones predicted by the model are the central ones, while those of lower and higher magnitude are closer to the estimated model values. A high value for the determination coefficient $(R^2 = 0.9613)$ was achieved.

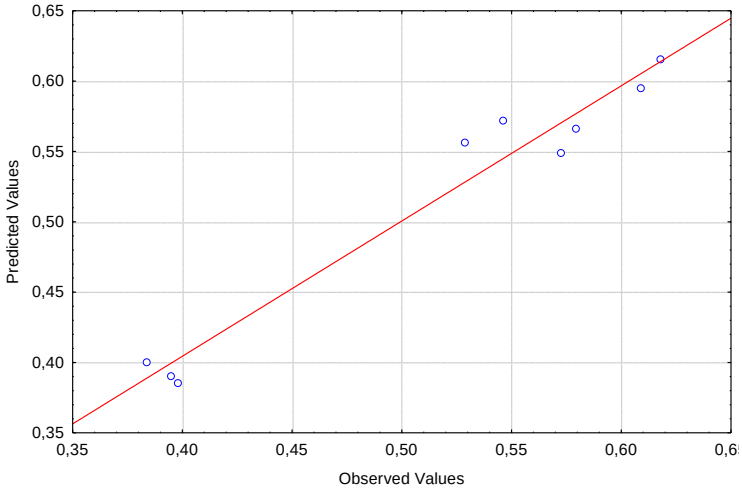

Figure 5.6: Observed vs predicted values.

$$FLS = 0.93 + 0.19H - 0.01H^2 - 1.06u_0 + 4.32{u_0}^2 - 0.12Hu_0 \quad (32)$$

In Table 5.5 are presented the experimental results, the predicted values, the error and the deviation of the results.

Analysing Table 5.5, it is visible that in the most of the cases the relative error of the results are lower than 5%. In the experiments performed with an inlet concentration of 100 mg/L, a bed depth comprehended between 2.5 and 7.5 cm and superficial velocities of 9.62 $x10^{-2}$ cm/s and 14.43$x10^{-2}$ cm/s, FLS is predicted with good accuracy by the model.

Table 5.5: Experimental results vs predicted results.

H (cm)	$u_o \times 10^2$ (cm/s)	Run	FLS experimental	FLS predicted	Relative error (%)
	9.62	1	0.384	0.400	4.36
2.5	14.43	2	0.398	0.385	3.11
	19.24	3	0.395	0.390	1.09
	9.62	4	0.609	0.595	2.34
5	14.43	5	0.579	0.566	2.35
	19.24	6	0.529	0.557	5.26
	9.62	7	0.618	0.615	0.40
7.5	14.43	8	0.546	0.572	4.76
	19.24	9	0.573	0.549	4.11

The surface response depicted in Figure 5.7, shows that the FLS is higher for higher bed heights and lower superficial velocity, as the Pareto chart suggests. Thus, analyzing the response surface plot generated by the predictive model is possible to identify the region of optimum values for the independent variables leading to maximization of the saturated bed fraction. An analytical optimal solution was found (H = 6.5 cm and u_o = 9.62x10^{-2} cm/s) using the MATLAB software to maximize FLS described by the model, in range of the tested variables. This means that this point corresponds to the global optimum which allows obtaining the maximum yield in the bed utilization, within defined ranges.

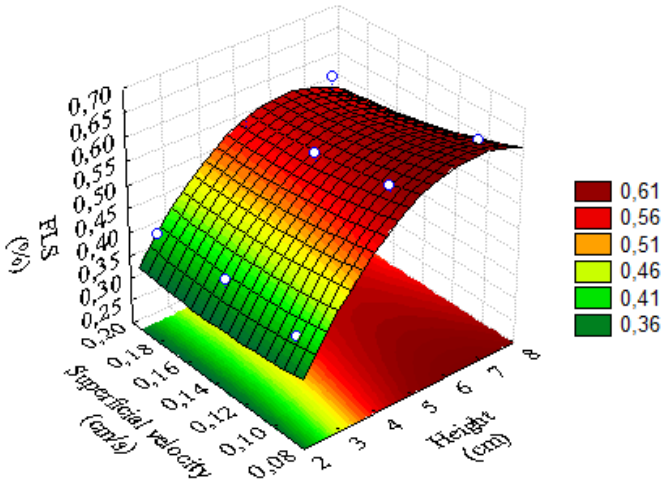

Figure 5.7: Three-dimensional response surface: effect of superficial velocity and height on the fraction of saturated bed (FLS).

On the second part, the same analyze was carried on with the goal was to minimize the difference between the exhaustion time and the breakthrough point, $\Delta t_{ads} = (t_E - t_{bp})$. In this case,

the response variable was Δt_{ads}, and the independent variables remained the same as in the previous study.

From the Pareto chart shown in Figure 5.8, it is possible to observe that the bed height remains the variable with higher impact on the response variable. However, the superficial velocity is also a significant variable which negatively affects Δt_{ads}, i.e. Δt_{ads} will take lower values when the superficial velocity increase.

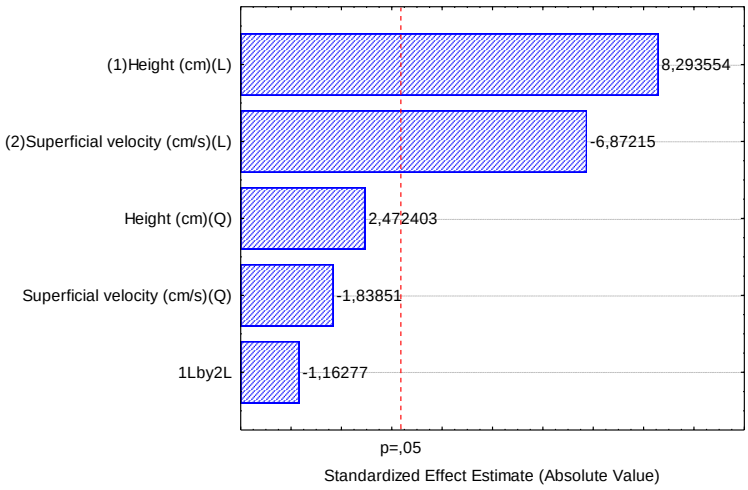

Figure 5.8: Pareto chart of the factors affecting Δt_{ads}.

The predictive model generated by the software is given by Equation (33). Analysing Fig. 5.9 it is noticeable that there is a good agreement between the experimental and model predicted values. For this case, the determination coefficient was of $R^2 = 0.9769$, which suggests that this model explains more accurately the results than the previous one.

$$\Delta t_{ads} = 168.19 + 64.25H - 3.71H^2 - 2601.14u_0 + \times 7444.98u_0^2 - 64.06Hu_0 \qquad (33)$$

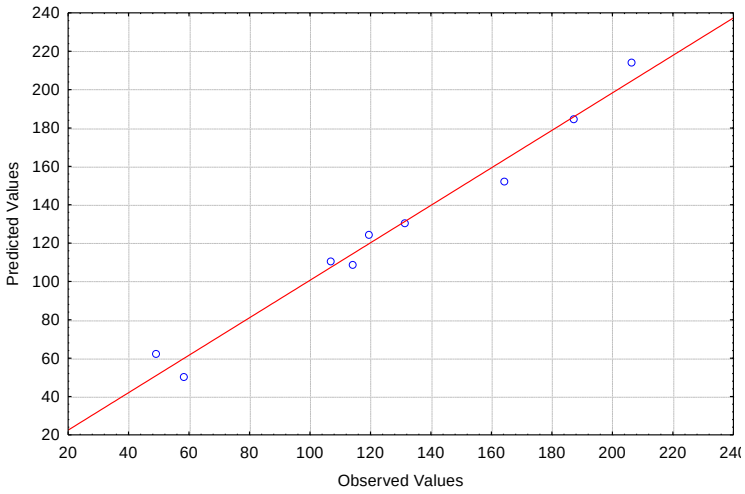

Figure 5.9: Observed vs predicted values.

Table 5.6 presents the experimental results, the predicted values, the error and the deviation of the results.

Table 5.6: Experimental results vs predicted results.

H (cm)	**$u_o \times 10^2$ (cm/s)**	**Run**	**Δt_{ads} real (min)**	**Δt_{ads} predicted (min)**	**Relative error (%)**
	9.62	1	114.01	108.91	4.48
2.5	14.43	2	48.89	62.22	27.26
	19.24	3	58.20	49.97	14.13
	9.62	4	187.28	184.64	1.41
5	14.43	5	131.20	130.24	0.73
	19.24	6	106.69	110.29	3.37
	9.62	7	206.29	214.04	3.76
7.5	14.43	8	164.31	151.94	7.53
	19.24	9	119.66	124.29	3.87

For this case, the relative error values shown in Table 5.6 for some experiments are relatively high when compared with the previous study (Table 5.5), even considering the goodness of fit of the model given by Eq. (33) with high R^2 value.

In this way, it is possible to observe that the model provides a better prediction for the experiments carried out with the bed depths of 7.5 and 5 cm. For those conducted on lower bed depth (2.5 cm), the model does not seem to have an accurate prediction since the predicted values possess a higher relative error associated.

Figure 5.10 depicts the three-dimensional response surface relationship between superficial velocity and the bed height on Δt_{ads}. This figure shows that the minimization of the difference between the exhaustion time and the breakthrough point occurs for the lower bed height values and higher superficial velocity. This means that under these conditions, the trend of the column saturation is closer to ideal conditions, compared to the experiments where the superficial velocity used is lower. It can also be concluded that the intraparticular diffusional effect has more importance in the cases where the solution is fed to the column at lower superficial velocities since the (t_E-t_{bp}) increases and the bed saturation takes longer.

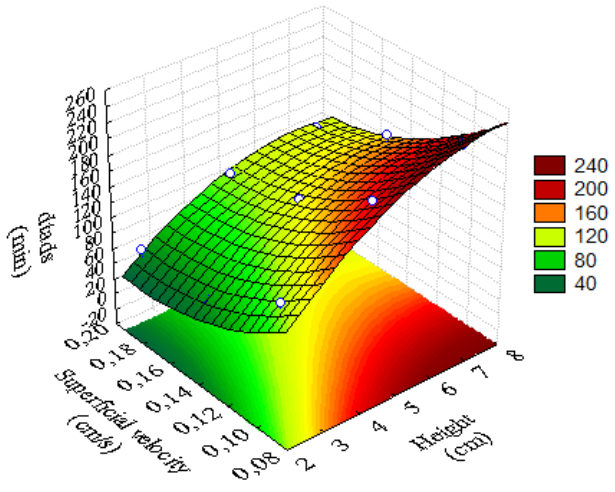

Figure 5.10: Three-dimensional response surface: effect of superficial velocity and height on Δt_{ads}.

5.4 Regeneration test

When the adsorbent reaches the saturation, i.e. equilibrium conditions are achieved, a regeneration step of the adsorbent may be crucially important to reduce the operation cost and to open the possibility of recovering the metal removed from the liquid phase by adsorption.

In previous batch studies[38], the desorption Cr(III) results showed that relatively high removal efficiencies were obtained using as regenerants the biodegradable complexing agent N,N-Bis(carboxymethyl)-DL-alanine trisodium salt (N,N-Bis at 50 ℃) and nitric acid (HNO_3 at 25 ℃). Therefore N, N-Bis and HNO_3 and were tested to regenerate the biosorbent preloaded with Cr(III).

The saturation experiments were performed with a bed depth of 6.5 cm and, superficial velocities of $9.62x10^{-2}$ cm/s (Run 12 before desorption with N,N-Bis) and $14.43x10^{-2}$ cm/s (Run

13 before desorption with HNO_3). In order to maximize FLS it was used a feed concentration of 100 mg/L. Figure 5.11 shows breakthrough curves corresponding to Runs 12 and 13.

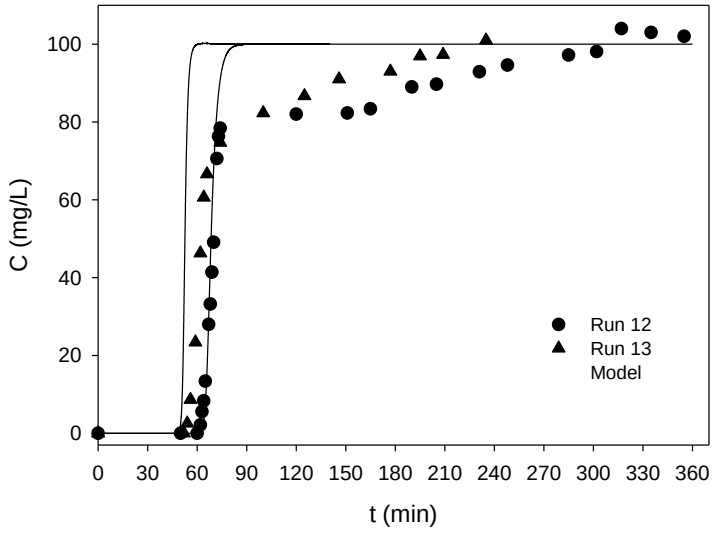

Figure 5.11: Experimental breakthrough curve (Run 12 and Run 13) and the data obtained by the simulated model.

The experimental breakthrough curves depicted in Fig. 5.11 were described by the mathematical model aforementioned and it is possible to observe that the model fits reasonably well the experimental values giving a good description of the dynamic response of the system. According to Table 5.7, the breakpoint time and the exhaustion time are 60.93 and 253.69 min for Run 12 and 52.78 and 185.50 min for Run 13. As might be expected, the lowest times are associated with the experiment conducted on high flow rate (Run 13). For these conditions, unexpectedly higher values of the adsorption capacity (q=32.57 mg/L) and FLS (0.65) were achieved. Regarding the q and FLS, for Run 12, the obtained values were similar to ones obtained in other experiments.

Table 5.7: Experimental results obtained from the saturation of the column.

Run	**H**	$\mathbf{u_o \times 10^2}$	$\mathbf{C_E}$	$\mathbf{t_{bp}}$	$\mathbf{t_E}$	$\mathbf{t_{st}}$	**q**	**FLS**	**τ**	$\mathbf{\Delta t_{ads}}$	**ξ**
	(cm)	**(cm/s)**	**(mg/L)**	**(min)**	**(min)**	**(min)**	**(mg/g)**		**(min)**	**(min)**	
12	6.5	9.62	100	60.93	253.69	97.33	30.42	0.62	0.35	192.76	275.85
13	6.5	14.43	100	52.78	185.50	80.17	32.57	0.65	0.23	132.72	341.01

With respect to regeneration, where the main goal is the recovery of metal ions adsorbed in the saturated biosorbent, thus giving the possibility of reusing it reducing the process cost, a possible Cr(III) desorption mechanism using acid as regenerant could be:[38]

$$(-RCOO)_2CrOH + 3H^+ \leftrightarrow 2(-RCOOH) + Cr^{3+} + H_2O \quad (34)$$

By the previous equation, it is possible to observe that during the desorption process, the H^+ ions take the place of the chromium ions present in the adsorbent, thus allowing their release and the possibility of regenerating the bed. The results of the regeneration tests are illustrated in Figure 5.12.

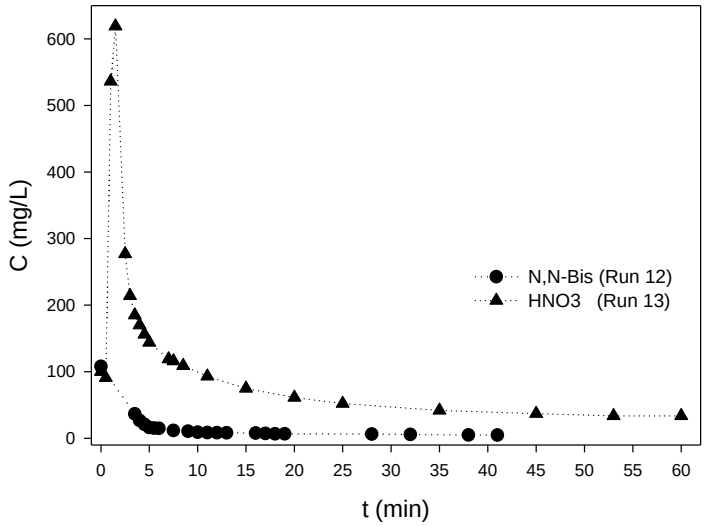

Figure 5.12: Desorption curves.

In order to determine the efficiency of the desorption, it was necessary to know the amount of chromium adsorbed by the MPB during the saturation step and the amount of Cr(III) desorbed during the regeneration. In Table 5.8 are present the both values, for the regeneration with N,N-Bis and HNO_3.

Table 5.8: Adsorbed and desorbed amount of chromium.

Run	**Total mass of chromium adsorbed, M_a (mg)**	**Total mass of chromium desorbed, M_d, (mg)**
12	97.34	5.49
13	104.22	48.83

Eq. (35) was used to calculate the desorption efficiency:

$$Desorption(\%) = \frac{M_d}{M_a} \times 100 \tag{35}$$

where M_d and M_a corresponds to the total amount of chromium desorbed and adsorbed (mg), respectively. M_d was calculated from the numerical integration of the regeneration curves.

A very low regeneration efficiency (5.6%) was observed when Cr(III) is eluted with N,N-Bis. This result was not expected since in batch studies the efficiency achieved was close to 43% A possible explanation to the lower value of efficiency could be due to the fact of the regenerative process with this complexing agent to be controlled by a very slow kinetics. In addition, the experiment duration (43 min) did not promote enough contact time between the regenerating agent and the sorbent to achieve an efficient desorption. Analysing Figure 5.12, it can be noticed that the behavior of the curve indicates that the desorption process was not as expected due to the absence of the typical 'peak', which corresponds to the fast release of the metal ions present in the adsorbent toward the effluent. In this way, the behavior of the curve for this case resembles more a bed washing.

The elution curve of chromium ions with (HNO_3) allowed determining a regeneration efficiency of 46.85%. This value still to be low and is not consistent with the result obtained from batch studies, where almost 82% of desorption was found. Figure 5.12 shows that for this case, there is the occurrence of a peak in the elution curve for Cr(III) where its concentration is about 6.2 times higher than the feed concentration (100 mg/L), used during the MPB saturation. This means that the regeneration of the bed with nitric acid promoted a fast desorption of the chromium ions from the adsorbent. After the elution to reach 10 min, the regeneration process becomes slower and controlled by dispersive effects, i.e. the curve exhibits a long tail, consequently, a long time will be needed to completely regenerate the adsorbent.

An increase in the (HNO_3) concentration in further desorption processes may be more effective in the removal of a larger amount of chromium ions from the biosorbent, however, the loss of biomass material can be significant. For the tested conditions, it was possible to calculate a material loss of 7.5% that also could have led contributed to a low removal efficiency. Thus, the possibility of the presence of another speciation of chromium in MPB, for the both cases, may influence their interactions with the eluent solution, reducing the efficiency removal.

5.5 Validation of the empirical models

To validate the previous empirical models developed by the software *Statistica7*, the experiments carried out to study the effect of the feed concentration (Run 10 and Run 11), as well as the pre-saturations for the regeneration tests (Run 12 and Run 13) were used. The Runs 10 and 11 were performed with optimal values of the bed height and superficial velocity (H=7.5 cm and $u_o= 9.62x10^{-2}$ cm/s) and where the concentration varied from 202 to 302 mg/L. For the saturation of the column before the regeneration tests, one of the experiments (Run 12) was

conducted under optimal conditions of H and u_o, analytically determined by the regression model used to maximize FLS, and the other experiment (Run 13) was performed using a bed depth of 6.5 cm and a superficial velocity of $14.43x10^{-2}$ cm/s.

Table 5.9: Experimental values vs predicted values for the model built for the case in which the FLS was considered as dependent variable.

Run	C_E (mg/L)	FLS experimental	FLS predicted	Relative error (%)
10	202	0.614	0.615	0.31
11	302	0.501	0.615	22.78
12	100	0.616	0.628	2.01
13	100	0.645	0.591	8.49

From Table 5.9 it is possible to conclude that the model provides a good prediction for the cases where the feed concentration was 202 mg/L (Run 10) and when the experiment was carried out with optimal values of the parameters (Run 12). However, the predicted FLS of the Run 11, has high relative error of 22.78%. Therefore, the model shows itself with a low predictive response for high Cr(III) feed concentrations.

In order to surpass this problem improving thus the robustness and precision of the model, another regression equation incorporating the solute concentration as an additional independent variable should be applied.

Table 5.10 shows the predicted results by the regression model considering $\Delta t_{ads} = (t_E - t_{bp})$ as the response variable. It is visible that the relative errors of the predicted values, are higher than ones found by using the previous model. As the inlet concentration increases the error associated with the predicted value for Δt_{ads} also increase, meaning that, as the previous case, the feed concentration affects the response estimated by the model. Relative error values of 29.60% and 54.34% were obtained for the Run 10 and Run 11, respectively.

Table 5.10: Experimental values vs predicted values for the model built for the case in which the (t_E-t_{bp}) was considered as dependent variable.

Run	C_E (mg/L)	Δt_{ads} experimental (min)	Δt_{ads} predicted (min)	Relative error (%)
10	202	165.16	214.04	29.60
11	302	138.68	214.04	54.34
12	100	192.76	207.84	15.08
13	100	132.72	148.82	12.13

For the case where it was used a feed concentration of 100 mg/L, Run 12 and Run 13, the relative error between the predicted and experimental values is lower compared to the other cases, however, it is still higher, taking the value of 15.08% and 12.13%, respectively.

In short, it can be concluded that both regression models appear to be very sensitive when subjected to variations in operational parameters that were not taking into account in the experimental design, such as feed concentration. However, the model that considers FLS as dependent variable provides better predicted values compared to the model in which Δt_{ads} was the response variable.

As previously mentioned, greater concentrations cause a higher gradient leading to a faster transport due to an increase diffusional coefficient. Moreover, given that fact the both models were obtained from an experimental design in which the inlet concentration was not taken into account as an independent variable, it was expected to get predicted values with high associated error, since the feed concentration significantly influences the dynamics of the adsorption process.

6. CONCLUSION AND FUTURE WORK

This study demonstrated that the adsorption process operated in a fixed bed column packed with mercerized pine bark have potential to be applied to the removal of Cr(III) ions from wastewaters, therefore be implemented in industrial processes.

It was demonstrated that the application of a Box-Benken design is an efficient tool to assess and optimize the process performance allowing a simultaneous evaluation of the response variables (FLS and Δt_{ads}) when the bed height and superficial velocities were changed.

The results obtained in the column studies showed that the uptake of chromium ions by MPB was dependent on the bed depth, superficial velocity and Cr(III) feed concentration. It was possible to observe that the adsorption capacity does not seem to vary significantly and the maximum value obtained was 35.35 mg/g. However, the metal uptake increased with the increasing of bed depth but decreased with the increase of the superficial velocity and inlet concentrations. Thus, it can be concluded that for an efficient column utilization, the adsorption process should be operated at lower superficial velocities, higher bed depths, and lower feed concentrations.

A mathematical model that incorporates the LDF approximation for describing the intraparticle transport was used to describe the dynamic behavior of the Cr(III) sorption in the column tests. A good agreement between model predictions and experimental data was achieved.

The statistical analysis of the results led to two regression models relating the independent variables (bed height and superficial velocity) and the variable response (FLS or Δt_{ads}). It also allowed to find which one of the operational parameters as more influence on the behavior of the system, according to the significance level obtained in the variance analysis. The best results were found with column operating at the following conditions: H = 6.5 cm and $u_o = 14.43 \times 10^{-2}$ cm/s, whose responses were FLS = 65% and $\Delta t_{ads} \approx 133$ min.

The FLS predicted values were well predicted, however, for the case of the Δt_{ads} the regression model was inaccurate since the predicted values were far from the experimental ones.

The regeneration tests using two regenerative agents (N,N-Bis and nitric acid) did not lead to an efficient elution of Cr(III) ions from the adsorbent since the removal efficiencies achieved were of 5.6% and 46.85 % with N,N-Bis and HNO_3, respectively.

However, since the adsorption process using fixed bed columns with agricultural residues still in a phase of research and development, technical and scientific issues should be solved to bring this technology into commercialization.

Based on this, future perspectives can be made:

- It is still essential to prepare more efficiently the MPB;
- In order to obtain accurate results, a real effluent should be used instead of a synthetic one;
- Many mathematical models are used for a single metal adsorption process; however, the elaboration of a new, improved, and simplified mathematical model is needed to get a better response comparing to the experimental results;
- Further attention should be given to the application of adsorption technology, using fixed bed columns, in product recovery-separation, purification, and recovery;
- At the industrial scale, economic analyses are required to obtain the overall cost of the adsorbent pre-treatment to purify a large quantity of wastewater.

REFERENCES

1. Barnhart, J. (1997). "Chromium chemistry and implications for environmental fate and toxicity". *Journal of Soil Contamination*. **6** ,561-568.
2. Fonseca-Correa, R., Giraldo, L., Moreno-Piraján, J.C. (2013). "Trivalent chromium removal from aqueous solution with physically and chemically modified corncob waste". *Journal of Analytical and Applied Pyrolysis.* **101**, 132-141.
3. Kurniawan, T.A., Chan, G.Y.S., Lo, W.H., Babel, S. (2006). "Physico-chemical treatment techniques for wastewater laden with heavy metals". *Chemical Engineering Journal*. **118**, 83-98.
4. Gupta, V.K., Carrott, P.J.M., Ribeiro-Carrott, M.M.L., Suhas. (2009). "Low-Cost Adsorbents: Growing Approach to Wastewater Treatment"—a Review. *Critical Reviews in Environmental Science and Technology*. **39**, 783-842.
5. Woodward, R.L. (1970). Environmental pollution. *Canadian Medical Association Journal*. **103**, 1316.
6. Su, C., Jiang, L., Zhang, W. (2014). "A review on heavy metal contamination in the soil worldwide: Situation, impact and remediation techniques". *Environmental Skeptics Critics*. **3**, 24-38.
7. Gunatilake, S.K. (2015). "Methods of Removing Heavy Metals from Industrial Wastewater". *Journal Multidisciplinary Engeineering Science Studies*. **1**, 2912-1309.
8. Barakat, M.A. (2011). "New trends in removing heavy metals from industrial wastewater". *Arabian Journal of Chemistry*. **4**, 361-377.
9. Kotasâ, J., Stasicka, Z. (2000). "Chromium occurrence in the environment and methods of its speciation". *Environmental Pollution*. **107**, 263–283.
10. Ayangbenro, A.S., Babalola, O.O. (2017). "A new strategy for heavy metal polluted environments: A review of microbial biosorbents". *International Journal of Environmental Research and Public Health*. **14**, 94.
11. Kumral, E. (2007). “Speciation of Chromium in Waters Via Sol-Gel Preconcentration Prior To Atomic Spectrometric Determination”. Master thesis submitted to School of engineering and Sciences of Ízmir Institute of Technology.
12. Vilar, V.J.P., Valle, J.A.B., Bhatnagar, A., et al. (2012). "Insights into trivalent chromium biosorption onto protonated brown algae Pelvetia canaliculata: Distribution

of chromium ionic species on the binding sites". *Chemical Engineering Journal*. **200-202**, 140-148.

13. Cossich, E.S., Da Silva, E.A., Tavares, C.R.G., Filho, L.C., Ravagnani, T.M.K. (2004). "Biosorption of chromium(III) by biomass of seaweed Sargassum sp. in a fixed-bed column". *Adsorption*. **10**, 129-138.

14. Fu, F., Wang, Q. (2011). "Removal of heavy metal ions from wastewaters: A review". *Journal of Environmental Management*. **92**, 407-418.

15. Lakherwal, D. (2014). "Adsorption of Heavy Metals: A Review" . *International Journal of Environmental Research and Development*. **4**, 41-48.

16. O'Connell, D.W., Birkinshaw, C., & O'Dwyer, T.F. (2008). "Heavy metal adsorbents prepared from the modification of cellulose: A review". *Bioresourcr Technology*. **99**, 6709-6724.

17. Bruch, L.W.; Cole, M. W., Zaremba, E. (1997). *Physical Adsorption: Forces and Phenomena*. 1st Edition. Clarendon Press. (ISBN: 0198556381**).**

18. Seader, J.D., Ernest, J. and Henlet, D. K. R. (2013). *Separation Process Principles* 3rd Edition. John Wiley & Sons. (ISBN: 9780470481837).

19. Ruthven, D.M. (1984). *Principles of Adsorption and Adsorption Processes*. Canada: John Wiley & Sons. (ISBN: 0471866067)

20. Geankoplis, C.J. (1993). *Transport processes and unit operations*. 3rd Edition. Prentice-Hall International, Inc. (ISBN: 013045253).

21. Thomas, W.J., Crittenden, B. (1998). *Adsorption Technology & Design*. Elsevier Science & Technology Books. (ISBN: 0750619597)

22. Pérez-Marín, A.B., Aguilar, M.I., Meseguer, V.F., Ortuño, J.F., Sáez, J., Lloréns, M. (2009). "Biosorption of chromium (III) by orange (Citrus cinensis) waste: Batch and continuous studies". *Chemical Engineering Journal*. **155**, 199-206.

23. Dabrowski, A. (2001). "Adsorption - From theory to practice". *Advances in Colloid and Interface Science*. **93**, 135-224.

24. Ali, I. (2014). "Water Treatment by Adsorption Columns: Evaluation at Ground Level". *Separation & Purification Review*. **43**, 175-205.

25. Ngah, W.S., Hanafiah, M.A.K.M. (2008). "Removal of heavy metal ions from wastewater by chemically modified plant wastes as adsorbents: A review". *Bioresource*

Technology. **99**, 3935-3948.

26. Ahmaruzzaman, M. (2011). "Industrial wastes as low-cost potential adsorbents for the treatment of wastewater laden with heavy metals". *Advances in Colloid and Interface Science*. **166**, 36-59.

27. Sud, D., Mahajan, G., Kaur, M.P. (2008). "Agricultural waste material as potential adsorbent for sequestering heavy metal ions from aqueous solutions - A review". *Bioresource Technology*. **99**, 6017-6027.

28. Pettersen, R.C. (1984) *The chemical composition of wood*: *The Chemistry of the solid wood*. American Chemical Society. Chapter 2, 1-9. (ISBN: 9780841207967).

29. Valentín, L., Kluczek-Turpeinen, B., Willför, S., et al. (2010). "Scots pine (Pinus sylvestris) bark composition and degradation by fungi: Potential substrate for bioremediation". *Bioresource Technology*. **101**, 2203-2209.

30. Bagyaraj, G.R.D.J. (1982). *Agricultural Microbiology*. New Delhi: Prentice-Hall of India. (ISBN: 9781483100333).

31. Thakur, V.K., Thakur, M.K., Gupta, R.K. (2014). "Review: Raw Natural Fiber–Based Polymer Composites". *International Journal of Polymer Analysis and Characterization*. **19**, 256-271.

32. Wertz, J. L., Bédué, O. and Mercier, J. P. (2010). *Cellulose Science and Technology*. Lausanne: EPFL Press. (ISBN 978-1-4398-0799-6).

33. Oudiani, A. E., Chaabouni. Y., Msahli, S., Sakli, F. (2011). "Crystal transition from cellulose i to cellulose II in NaOH treated Agave americana L. fibre". *Carbohydrate Polymers*. **86**, 1221-1229.

34. Hill C.A.H. (2006). *Wood Modification: Chemical, Thermal and Other Processes*. Christian V. Stevens. (ISBN: 978-0-470-02172-9).

35. Miranda, I., Gominho, J., Mirra, I., Pereira, H. (2012). "Chemical characterization of barks from Picea abies and Pinus sylvestris after fractioning into different particle sizes". *Industrial Crops Products*. **36**, 395-400.

36. De Gisi, S., Lofrano, G., Grassi, M., Notarnicola, M. (2016). "Characteristics and adsorption capacities of low-cost sorbents for wastewater treatment: A review". *Sustainable Materials and Technology*. **9**, 10-40.

37. Demirbas, A. (2008). "Heavy metal adsorption onto agro-based waste materials: A

review". *Journal of Hazardardous Materials*. **157**, 220-229.

38. Arim, A.L., Cecílio, D.F.M., Quina, M.J., Gando-Ferreira, L.M. (2018). "Development and characterization of pine bark with enhaced capacity for uptaking Cr(III) from aqueous solutions". *Canadian Journal of Chemical Engineering*. (in press).

39. Ofomaja, A.E., Naidoo, E.B., Modise, S.J. (2009). "Removal of copper(II) from aqueous solution by pine and base modified pine cone powder as biosorbent". *Journal of Hazardous Materials*. **168**, 909-917.

40. Gurgel, L.V.A., Gil, L.F. (2009). "Adsorption of Cu(II), Cd(II) and Pb(II) from aqueous single metal solutions by succinylated twice-mercerized sugarcane bagasse functionalized with triethylenetetramine". *Water Research*. **43**, 4479-4488.

41. McCabe, W. L., Smith, J., Harriot, P. (1993) *Unit operations of chemical engineering*. 5th Edition. International Editions. (ISBN:0071127380).

42. Moreno-Pirajan, J. et al. (2006). "Scale-up of pilot plant for adsortion of heavy metals". *An. Asoc. Quím. Argent.* **94**, 71-82.

43. Green, D. W., Perry, R. H. (2007). *Perry's Chemical Engineers' Handbook*. 8th Edition. McGraw-Hill Education. (ISBN: 978-0071422949).

44. Cecílio, D.F.M. (2016). "Treatment of an effluent polluted with Cr (III) by adsorption onto chemically modified agro-industrial waste". Master thesis submitted to Department of Chemical Engineering of University of Coimbra.

45. Wankat, P. (1994). *Rate-Controlled Separations*. Chapman and Hall. (ISBN: 9780751402841).

46. Xu, Z., Cai, J., Pan, B. (2013). "Mathematically modeling fixed-bed adsorption in aqueous systems". *Journal of Zhejiang University- Science A*. **14**, 155-176.

47. Dym, C. (2004). *Principles of Mathematical Modeling*. 2nd Edition. Academic Press. (ISBN: 9780080470283).

48. Du, X., Yuan, Q., Li, Y. (2008). "Mathematical analysis of solanesol adsorption on macroporous resins using the general rate model. *Chemical Engineering & Technology*. **31**, 1310-1318.

49. Eldestein-Keshet, L. (2005). *Mathematical Models in Biology*. Society for Industrial and Applied Mathematics Philadelphia. (ISBN: 0898715547).

50. De Almeida, A.M. (2012). "Estudo numérico de colunas de adsorção de leito fixo".

Master thesis submitted to University Federal do Paraná, Sector of Technology.

51. Hatzikioseyian, A., Mavituna, F., Tsezos, M. (1999). "Modelling of fixed bed biosorption columns in continuous metal ion removal processes. The case of single solute local equilibrium". *Process Metallurgy*. **9**, 429-448.

52. Luz, A.D. (2012). "Aplicação de coluna de adsorção em leito fixo para a remoção de compostos BTX multicomponentes presentes em efluentes petroquímicos". Master thesis submitted to Department of Chemical Engineering of University Federal de Santa Catarina.

53. Otero, M., Zabkova, M., Rodrigues, A.E. (2005). "Phenolic wastewaters purification by thermal parametric pumping: Modeling and pilot-scale experiments". *Water Resources*. **39**, 3467-3478.

54. Glueckauf, E. (1955). Theory of chromatography. Part 10. Formulae for diffusion into spheres. *Trans Faraday Society*. **51**, 1540-1554.

55. Gando-Ferreira, L.M., Romão, I.S., Quina, M.J. (2011). "Equilibrium and kinetic studies on removal of Cu2+ and Cr3+ from aqueous solutions using a chelating resin". *Chemical Engineering Journal*. **172**, 277-286.

56. Chu, K.H. (2004). "Improved fixed bed models for metal biosorption". *Chememical Engineering Journal*. **97**, 233-239.

57. Tofan, L., Paduraru, C., Teodosiu, C., Toma, O. (2015). "Fixed bed column study on the removal of chromium (III) ions from aqueous solutions by using hemp fibers with improved sorption performance". *Cellulose Chemistry and Technology*. **49**, 219-229.

58. Calero, M., Hernáinz, F., Blázquez, G., Tenorio, G., Martín-Lara, M.A. (2009). "Study of Cr (III) biosorption in a fixed-bed column". *Journal of Hazardous Materials*. **171**, 886-893.

59. Veit, M.T., Silva, E.A., Fagundes-Klen, M.R., Tavares, C.R.G., Gonçalves, G.C. (2008). " Biosorption of chromium(III) in fixed bed column". *Estudos tecnológicos*. **4**, 88-104.

60. Tofan, L., Teodosiu, C., Paduraru, C., Wenkert, R. (2013). "Cobalt (II) removal from aqueous solutions by natural hemp fibers: Batch and fixed-bed column studies". *Applied Surface Science*. **285**, 33-39.

61. Da Silva, E.A., Cossich, E.S., Tavares, C.R.G., Filho, L.C., Guirardello, R. (2002). "Modeling of copper(II) biosorption by marine alga Sargassum sp. in fixed-bed column".

Process Biochemistry. **38**, 791-799.

62. Taty-Costodes, V.C., Fauduet, H., Porte, C., Ho, Y.S. (2005). "Removal of lead (II) ions from synthetic and real effluents using immobilized Pinus sylvestris sawdust: Adsorption on a fixed-bed column". *Journal of Hazardous Materials*. **123**, 135-144.

63. Malkoc, E., Nuhoglu, Y.(2005) "Removal of Ni(II) ions from aqueous solutions using waste of tea factory: Adsorption on a fixed-bed column". *Journal of Hazardous Materials*. **135**, 328-336.

64. Tien, C. (1994). *Adsorption Calculations and Modeling*. Boston: Butterworth-Heinemann. (ISBN: 0750691212).

65. Liu, B., Zeng, L., Mao, J., Ren, Q. (2010). "Simulation of levulinic acid adsorption in packed beds using parallel pore / surface diffusion model. *Chemical Engineering & Technology*. **33**, 1146-1152.

66. Ko, D.C.K., Porter, J.F., McKay, G. (2005). "Application of the concentration-dependent surface diffusion model on the multicomponent fixed-bed adsorption systems". *Chemical Engineering Science.* **60**, 5472-5479.

67. Helfferich, F.G., Carr, P.W. (1993). "Non-linear waves in chromatography. I. Waves, shocks, and shapes". *Journal of Chromatogr*. **629**, 97-122.

68. Chern, J., Chien, Y. (2001). "Adsorption isotherms of benzoic acid onto activated carbon and breakthrough curves in fixed-bed columns. *Water Research.* **36**, 3775-3780.

69. Clark, R.M. (1987). "Evaluating the Cost and Performance of Field-Scale Granular Activated Carbon Systems". *Environmental Science and Technology*. **1**,573-580.

70. Hutchins R. (1973). "New method simplifies design of activated carbon systems". *Chemical Engineering*. **80,** 133-138.

71. Yoon,Y.H., Nelson, J.H. (1984). "Application of Gas Adsorption Kinetics I. A Theoretical Model for Respirator Cartridge Service Life". *American Industrial Hygiene Association Journal*. **45**, 509-16.

72. Title, S., Title, C., et al. (2013). "Drug Delivery Systems: Advanced Technologies Potentially Applicable in Personalised Treatment". **3**,4.

73. Brouwer P. (2010). *Theory of XRF*. 3rd Edition. PANalytical BV, The Netherlands. (ISBN: 9090167587).

74. Heckert, N.A., Filliben, J.J., Croarkin, C.M., Hembree, B., Guthrie, W.F., Tobias, P.,

Prinz, P. (2002). *Engineering Statistics e-Handbook.*

75. Han, R., Zou, L., Zhao, X., et al. (2009). "Characterization and properties of iron oxide-coated zeolite as adsorbent for removal of copper(II) from solution in fixed bed column". *Chemical Engineering Journal*. **149**, 123-131.

7. APPENDIXES

7.1 Appendix A- Particle size distribution

In the Figure A.1 it is possible to observe the particle size distribution of the MPB used in this project.

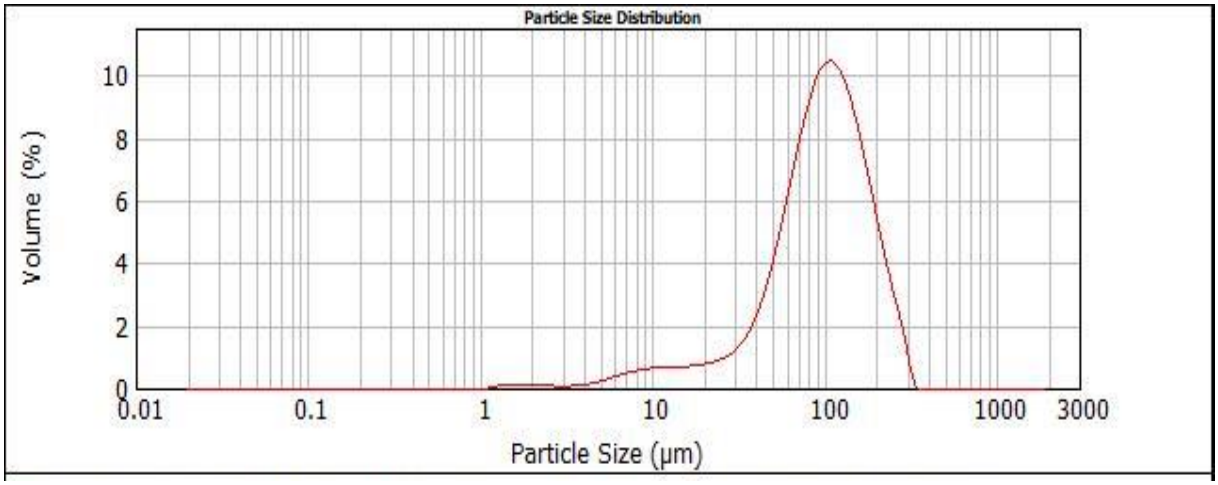

Figure A.1: Experimental data for the particle size distribution of MPB.

7.2 Appendix B- Experimental data

On the following Tables are present the experimental values obtained from the column experiments for each case study.

Table B.1: Experimental data for the bed depth of 2.5 cm using different superficial velocities.

$9.62x10^{-2}$ cm/s		**$14.43x10^{-2}$ cm/s**		**$19.24x10^{-2}$ cm/s**	
t (min)	C (mg/L)	t (min)	C (mg/L)	t (min)	C (mg/L)
0	0	0	0	0	0
10	0	10	0	8	0
26	0	13	0	10	0
28	1,02	15	3,93	11	3,62
29	4,15	16	7,36	12	7,42
31	12,9	17	12,7	13	15,1
33	25,5	18	20,5	14	22
34	33,3	20	41,2	16	41,6
35	42,1	21	52,4	17	53,9
36	50,1	22	59,7	18	59,1
37	55,2	23	67,2	19	66,2
39	66,1	24	71,6	20	71,3
40	69	25	79,3	21	75,1
41	71,4	28	86,1	22	77,3
42	72,7	32	90,3	23	82
43	73	36	91,8	24	83,2
44	74	45	91,9	26	87,6
46	75,3	50	92,1	27	89,2
48	77	55	93,3	30	90,1
50	78,1	65	94,7	36	90,3
60	84,6	90	95,8	43	92,3
64	85,7	131	96,2	50	93,1
74	87,9	163	96,5	60	93,3
91	92,7	192	96,8	67	94,1
108	93,9	204	97,1	72	94,9
129	94	215	97,3	85	95,4
139	94,6	221	98,1	102	96,5
164	96,6	230	99,8	122	97,2
176	96,7	238	100	134	99
191	97,1			143	100
203	97,9				
247	101				
268	102				

Table B.2: Experimental data for the bed depth of 5 cm using different superficial velocities.

$9.62x10^{-2}$ cm/s		**$14.43x10^{-2}$ cm/s**		**$19.24x10^{-2}$ cm/s**	
t (min)	C (mg/L)	t (min)	C (mg/L)	t (min)	C (mg/L)
0	0	0	0	0	0
45	0	20	0	10	0
49	0	30	0	20	0,0505
50	1,33	31	1,82	21	3,16
51	3,23	32	4,5	22	6,53
52	6,62	33	7,28	23	11,5
53	11,6	34	11,3	24	17,8
55	19,6	35	18,3	25	30,1
56	26,9	36	28,2	26	42,8
57	33,3	37	34,9	27	55,1
58	39,4	38	44,5	28	62,7
59	47,2	39	53,1	29	67,7
60	56,6	40	59,8	30	69,9
61	61,1	41	63,4	31	73,9
63	65,9	42	65,8	33	77,1
65	69,8	43	69,9	34	79,7
67	71,1	47	79,3	35	83,3
72	75,7	52	83,9	36	86
74	79,5	60	86,4	39	87,5
79	81,2	71	88,1	42	88,7
89	81,8	76	89,4	50	90,5
103	83,8	81	90	53	90,7
143	88,7	90	91,5	56	91,2
185	92,3	100	92,3	69	91,3
207	92,4	120	93,5	83	92,8
227	93,1	133	94,8	92	94,1
246	95,8	168	96,2	120	94,7
270	97,1	179	97,4	134	95,3
295	100	201	101	143	95,8
305	99,6	217	100	169	97
		226	101	181	98,1
				206	99,8
				217	100
				224	101

Table B.3: Experimental data for the bed depth of 7.5 cm using different superficial velocities.

$9.62x10^{-2}$ cm/s		**$14.43x10^{-2}$ cm/s**		**$19.24x10^{-2}$ cm/s**	
t (min)	C (mg/L)	t (min)	C (mg/L)	t (min)	C (mg/L)
0	0	0	0	0	0
10	0	5	0	5	0
40	0	10	0	10	0
60	0	20	0	20	0
70	0	30	0	30	0
81	0,778	38	0	32	0
84	6,04	43	0	34	1,22
86	11,7	49	21,1	36	6,77
88	18,2	52	37,8	38	14,6
90	24,8	54	51	40	26,7
92	35,7	56	65,9	43	55
94	45,3	93	84,4	44	63,5
96	54,2	98	85	46	71,2
98	60,1	116	85,2	48	73,8
100	66	134	85,2	50	75,1
104	69,7	165	86,3	52	76,2
110	71,7	182	88	54	77
140	81	198	89,1	56	78,1
147	82,4	209	92,6	87	86,2
159	86,6	223	96,7	113	87,6
180	89,2	231	97,5	123	88,9
202	89,3			139	92,5
225	90			160	94,5
237	91,4			175	97,1
257	92,3			196	98,3
300	93,7				
315	93,8				
336	93,9				
345	94,5				
360	95,8				

Table B.4: Experimental data for the bed depth of 7.5 cm and superficial velocity of $9.62x10^{-2}$ cm/s using different feed concentrations.

100 mg/L		**200 mg/L**		**300 mg/L**	
t (min)	C (mg/L)	t (min)	C (mg/L)	t (min)	C (mg/L)
0	0	0	0	0	0
70	0	38	0	24	0
81	0,778	39	1,1	25	1,99
84	6,04	40	6	26	10,5
86	11,7	41	16,9	27	25,7
88	18,2	42	34,3	28	47,6
90	24,8	43	52,5	29	82,7
92	35,7	44	75,6	30	126
94	45,3	45	101	31	174
96	54,2	46	122	32	215
98	60,1	47	143	33	239
100	66	48	157	34	252
104	69,7	49	166	49	261
110	71,7	50	170	82	262
140	81	51	172	90	263
147	82,4	52	174	110	265
159	86,6	54	177	120	267
180	89,2	57	178	129	271
202	89,3	141	180	140	275
225	90	174	186	150	281
237	91,4	210	193	160	285
257	92,3	230	194	170	290
300	93,7	250	195	185	295
315	93,8	265	200	210	298
336	93,9	275	205	215	300
345	94,5	310	208	220	303
360	95,8	315	206	235	302
380	95,5				
405	98,4				

Table B.5: Experimental data for saturation of the column for the regeneration tests.

$9.62x10^{-2}$ cm/s		**$14.43x10^{-2}$ cm/s**	
t (min)	C (mg/L)	t (min)	C (mg/L)
0	0	0	0
50	0	52	0
60	0	54	2,57
62	2,14	56	8,66
63	5,59	59	23,4
64	8,34	62	46,3
65	13,4	64	60,6
67	28	66	66,6
68	33,2	74	74,7
69	41,4	100	82,3
70	49,1	125	86,7
72	70,6	146	91
73	76,3	177	93
74	78,4	195	96,9
120	82	209	97,3
151	82,3	235	101
165	83,4		
190	89		
205	89,7		
231	92,9		
248	94,6		
285	97,2		
302	98,1		
317	104		
335	103		
355	102		

Table B.6: Experimental data for the regeneration tests.

N, Nbis		**HNO_3**	
t (min)	C (mg/L)	t (min)	C (mg/L)
0	108,0	0	100
3,5	36,6	0,5	90,8
4,	26,8	1	536
4,5	21	1,5	619
5	16,18	2,5	277
5,5	15,32	3	214
6,	14,92	3,5	185
7,5	11,78	4	170
9,	10,62	4,5	156
10	9,02	5	144
11	8,48	7	119
12	8,38	7,5	116
13	8,14	8,5	109
16	7,86	11	93,2
17	7,28	15	74,8
18	6,7	20	61,2
19	6,6	25	52,1
28	6,34	35	41,9
32	5,7	45	37,1
38	5,06	53	33,7
41	4,74	60	33,7